Anti-CD19 CAR T cells potently redirected to kill solid tumor cells

Christine Ambrose[1], Lihe Su[1], Lan Wu[1], Fay J. Dufort[1], Thomas Sanford[1], Alyssa Birt[1], Benjamin Hackel[2], Andreas Hombach[3], Hinrich Abken[3,§], Roy R. Lobb[1] and Paul D. Rennert[1*].

1: Aleta Biotherapeutics, Natick, MA USA.

2: University of Minnesota, Minneapolis, MN USA.

3: University of Cologne, Köln, Germany.

* Correspondence should be addressed to P.D.R (paul.rennert@aletabio.com)

§ current address: Regensburg University, Regensburg, Germany.

CAR-CD19 T cells used to target solid tumors

Abstract

Successful CAR T cell therapy for the treatment of solid tumors requires exemplary CAR T cell expansion, persistence and fitness, and the ability to target tumor antigens safely. Here we address this constellation of critical attributes for successful cellular therapy by using integrated technologies that simplify development and derisk clinical translation. We have developed a CAR-CD19 T cell that secretes a CD19-anti-Her2 bridging protein. This cell therapy strategy exploits the ability of CD19-targeting CAR T cells to interact with CD19 on normal B cells to drive expansion, persistence and fitness. The secreted bridging protein potently binds to Her2-positive tumor cells, mediating CAR-CD19 T cell cytotoxicity *in vitro* and *in vivo*. Because of its short half-life, the secreted bridging protein will selectively accumulate at the site of highest antigen expression, ie. at the tumor. Bridging proteins that bind to multiple different tumor antigens have been created. Therefore, antigen-bridging CAR-CD19 T cells incorporate critical attributes for successful solid tumor cell therapy. This platform can be exploited to attack tumor antigens on any cancer.

Introduction

The treatment of relapsed or refractory Acute Lymphocytic Leukemia (ALL) and Non-Hodgkin Lymphoma (NHL) with chimeric antigen receptor (CAR) T-cells that target CD19 (CAR-CD19 T cells) has led to FDA and EMA approvals of the adoptive cell therapies tisagenlecleucel and axicabtagene ciloleucel [1, 2]. CAR-CD19 T cells have thus paved the way for the development of cellular therapeutics as 'living drugs', and have driven our understanding of CAR T cell regulatory, CMC and commercialization issues [3]. Furthermore, CAR-CD19 T cells are routinely used to evaluate all aspects of CAR T cell function, including optimization of signaling domains and hinge regions [4], development of dual CARs [5, 6], expression of cytokines, antibodies, and other mediators [7, 8], evaluation of toxicities [9, 10], and of switch technologies [11, 12]. CAR-CD19 T cells also provide a simple and universal solution to the issue of CAR T cell persistence. Robust *in vivo* expansion followed by prolonged CAR-T cell persistence is critical for their efficacy in the treatment of hematologic malignancies [13, 14]. Since CD19-positive normal B cells are constantly produced by the bone marrow in response to B cell depletion, CAR-CD19 T cells uniquely access a non-tumor dependent and self-renewing source of activating antigen. This is true even in patients who have undergone lymphodepleting chemotherapy as the bone marrow can recover and start producing B cells in as little as 28 days [15, 16]. In contrast, other CAR T cells, particularly those targeting solid tumor antigens, have largely shown poor persistence to date [17]. In short, CAR-CD19 T cells have properties which make them uniquely suited to CAR T cell therapy, come with a broad and expanding set of pre-clinical knowledge and possess an unmatched development history.

To capitalize on this deep knowledge base, we have chosen to use CAR-CD19 T cells as a unique platform solution that will allow us to target and kill any tumor. We recently described the development of bridging proteins which contain the extracellular domain (ECD) of CD19 linked to an antigen binding domain, eg. an antibody fragment, that binds to a tumor-expressed antigen [18]. The wild-type CD19 ECD was difficult to express, therefore we developed novel CD19 ECD mutants that can be linked N- or C-terminally to any protein, generating modular CD19 bridging proteins with enhanced secretion and a predicted lack of immunogenicity [18]. These rationally designed CD19 bridging proteins are capable of binding to any tumor antigen, thereby coating CD19-negative tumor cells with CD19. CD19-coated tumor cells representing diverse indications were thereby made susceptible to potent CAR-CD19 T cell-mediated cytotoxicity [18]. Of note, the CAR-CD19 domain on the T cell remains the same regardless of the antigens targeted by the bridging protein, and this minimizes complexity in CAR T cell manufacturing across our diverse programs. This technology therefore has the potential to broaden the reach of CAR-CD19 T cells beyond B cell malignancies to any tumor without the need to build many different CAR and combination CAR constructs. Given the emerging knowledge regarding the need for multi-antigen targeting in order to ensure durable responses to CAR-T therapy the need for such a simple, pragmatic and modular technology is evident.

Here we describe the use of CAR-CD19 T cells that secrete CD19 bridging proteins as a highly effective therapeutic approach to targeting hematologic cancers and solid tumors. CD19 bridging proteins are simple and modular solutions to multi-antigen targeting, antigen selectivity, and optimization of potency and safety. This technology retains the inherent advantages of CAR-CD19 T cells and leverages the development and manufacturing knowledge accumulated to date.

Results

CD19-anti-Her2 bridging proteins bind with high affinity to anti-CD19 and to Her2

We have previously shown that wildtype and stabilized forms of the CD19 ECD can be fused to a variety of scFvs, VHHs, and scaffold proteins such as Fibronectin Type III (Fn3) domains, with the retention of binding function, CAR-CD19 recognition and cytotoxicity [18, 19]. These CD19-containing proteins bind to both CAR-CD19 T cells and to the targeted tumor antigens, and are referred to as bridging proteins. Here we show that bridging proteins can be secreted by CAR-CD19 T cells transduced with a lentiviral vector construct that encodes both a cell surface CAR-CD19 sequence and a bridging protein sequence. Functionally, bridging proteins act as CAR T engagers, activating the CAR T cell and killing the bound tumor cell (Fig 1).

Figure 1. **Schematic representation of the technology.** A) A lentiviral expression vector was created that encodes an anti-CD19 CAR domain, a 2A cleavage site, and a secreted CD19-anti-Her2 scFv bridging protein. B) Human primary T cells were transduced and expanded. C) The T cell transduction resulted in the expression of the anti-CD19 CAR domain on the T cell surface (thus, CAR-CD19) and secretion of the bridging protein. D) The bridging protein has two domains: the anti-Her2 scFv bound to Her2 expressed on the tumor cell; the CD19 ECD bound to the anti-CD19 CAR domain on the transduced T cell. Thus the bridging protein acts as a CAR-T cell engager protein. E) The binding events created a cytotoxic immune synapse between the CAR-CD19 T cell and the Her2-positive tumor cell via recognition of CD19; this resulted in CAR T cell proliferation and tumor cell death.

A bridging protein containing the wildtype CD19 ECD sequence and the anti-Her2 scFv was described previously [18]. Novel, stabilized forms of the CD19 ECD were also described previously [18] and one of these ($CD19_{C6.2}$) was used to create a CD19-anti-Her2 bridging protein (construct #340, Table 1). The most important difference in the two forms of the CD19 ECD used is the level of protein expression from transfected cells that these support; the stable form also binds more tightly to the anti-CD19 scFv from the FMC63 monoclonal antibody [18]. Several proteins were created as specificity controls, containing just the CD19 ECD or containing a CD22 ECD linked to the anti-Her2 scFv (constructs #28 and #117, Supplemental Table 1).

Table 1. List of major constructs used in the text. Constructs are presented in the numerical order with a description of the encoded sequences in column 2 and the format in which the expressed sequence is utilized in column 3. The long dashes indicate a linker sequence. P2A refers to a cleavage sequence. BP refers to a bridging protein.

Construct #	Description	Modality
254	CAR sequence targeting CD19	Anti-CD19 CAR
340	Stabilized CD19 ECD – anti-Her2	Purified BP
374	Sequence of 254 – P2A – sequence of 340	Anti-CD19 CAR + stabilized BP
390	CAR sequence targeting Her2	Anti-Her2 CAR
460	Anti-Her2 – stabilized CD19 ECD – anti-EGFR	Purified BP

We characterized the binding properties of CD19-anti-Her2 bridging proteins. In ELISA assays CD19-bridging proteins were shown to bind both to the anti-CD19 antibody FMC63 and to the Her2 antigen with low nM affinity (Table 2, Supplemental Fig 1a,b). We then examined binding to T cells expressing the anti-CD19 CAR domain. Donor human T cells were transduced with lentiviral particles that express the scFv derived from the anti-CD19 antibody FMC63 (CAR-CD19, construct #254, Table 1). Transduced T cells expressed the anti-CD19 CAR domain as detected with anti-Flag antibody staining (Supplemental Fig 2a). We performed a flow cytometry assay to assess the binding of the CD19-anti-Her2 bridging proteins (#340, Table 1; #42, Supplemental Table 1) to anti-CD19 CAR T cells. CD19-anti-Her2 bridging proteins bound to CAR-CD19 T cells with a low nM affinity but did not bind to control (un-transduced, UTD) T cells (Table 2, Supplemental Fig 2b). In the linear range of the assay (approximately 0.5 – 100 ng/ml) the bridging protein having a stabilized CD19 ECD (#340) demonstrated statistically superior binding (Supplemental Figure 2b), consistent with previous results [18].

Table 2. Summary of bridging protein binding and cytotoxicity data. Data are reported as mean +/- standard error. ELISA assay data were produced from triplicate wells, flow cytometry assay data were produced in duplicate, and cytotoxicity assay data were produced in triplicate. The number of repeats ('n') per experiment is shown for each assay. Top: EC_{50} binding data for bridging proteins and control proteins as determined in ELISA assays. The capture reagents, detection reagents and protein construct numbers are indicated. Middle: EC_{50} binding data for bridging proteins and control proteins as determined in flow cytometric assays. The cells used are indicated. Flow cytometry reagents used to detect cell-bound proteins were anti-CD19 antibody FMC63 (#42, #340, #28) or anti-His tag antibody (#117). Bottom: bridging protein-

mediated CAR-CD19 cytotoxicity against Her2-positive cell lines. CAR-CD19 T cells from donor 54 (47% CAR-positive) and donor 69 (54% CAR positive) were used at an E:T ratio of 10:1. IC_{50} values were derived from a titration of the bridging protein concentration in the assays. For all assays shown, 'none' indicates that no binding or activity above background was detected; a '-' indicates that the experiment was not performed.

Bridging protein binding affinity in ELISA assays (EC_{50})					
CAPTURE	**DETECTION**	**#42**	**#340**	**#28**	**#117**
FMC63	Her2	0.2 +/- 0.18 nM n=2	0.06 +/- 0.03 nM n=2	none n=2	none n=2
Her2-Fc	FMC63	0.35 +/- 0.26 n=2	0.19 +/- 0.04 n=2	none n=2	none n=1
Bridging protein binding affinity in flow cytometric assays (EC_{50})					
Cells	CAR-CD19 T cells	0.6 +/- 0.12 nM n=2	0.21 +/- 0.01 nM n=2	-	-
	untransduced T cells	none n=2	none n=2	-	-
	SKOV3	1.2 +/- 0.74 nM n=7	1.5 +/- 1.1 nM n=2	none n=3	0.68 +/- 0.32 nM n=2
	BT474	0.26 +/- 0.3 nM n=3	0.24 +/- 0.3 nM n=3	none n=2	0.45 nM n=1
Bridging protein mediated cytotoxicity (IC_{50})					
Donor	**Target cells**	**#42**	**#340**	**#28**	**#117**

54/69	SKOV3	4.8 +/- 2.7 pM n=14	4.7 +/- 2.6 pM n=2	none n=2	none n=1
54/69	BT474	12.2 +/- 3.6 pM n=2	7.4 +/- 0.3 pM n=2	none n=2	-

SKOV3 ovarian carcinoma cells and BT474 breast carcinoma cells express Her2 (Supplemental Fig 2c). Flow cytometry assays using Her2-positive SKOV3 and BT474 cells demonstrated that the purified CD19-anti-Her2 bridging proteins consistently bound with low nM EC_{50} values, ranging from 0.2 – 2.7 nM (Table 2; Supplemental Fig 2d). In this binding format the bridging proteins were indistinguishable from each other, as expected given that they use the same anti-Her2 scFv from trastuzumab. These data showed that both halves of the CD19-anti-Her2 bridging protein were fully functional, binding to the CAR expressing the anti-CD19 FMC63 scFv and to the Her2 antigen on the SKOV3 cell surface. The control CD22-anti-Her2 bridging protein bound to Her2-positive SKOV3 cells, but the CD19 ECD protein failed to bind to either SKOV3 cells or BT474 cells (Table 2, Supplemental Figure 3). These data further illustrate the specificity of the binding components within bridging proteins.

Next we turned to experiments utilizing the bridging proteins and anti-CD19 CAR T cells. In all experiments the effector to target ratio is calculated by the total number of T cells, not the number of CAR-positive T cells. Therefore the donor number and positive CAR percentage for each experiment is stated.

CD19-anti-Her2 does not compromise CAR-CD19 function

To address the potency of direct cytotoxicity via CD19 binding, CAR-CD19 T cell activity was determined at different effector:target (E:T) ratios using the CD19-positive B cell line Nalm6. The CAR construct used is a generation 3 design (with 4-1BB/CD28/CD3 cytoplasmic components) and uses the FMC63 scFv (see Methods). The flow cytometry methods used to characterize anti-CD19 CAR T cells after transduction and expansion are shown (Figure 2a, donor 45). Cytotoxicity was routinely observed down to the lowest E:T ratio tested, although there was some variation in the extent of cytotoxicity depending on the specific normal human donor T cells used in the assay (Fig 2b).

Aberrant signaling can drive CAR T cells into a dysfunctional state [20]. Therefore we assessed the impact of binding the CD19-anti-Her2 bridging protein (#340) on CAR-CD19 T cell cytotoxicity against the target cell lines Nalm6 (CD19-positive) and SKOV3 (Her2-positive). Cytotoxicity against Nalm6 cells requires that the anti-CD19 CAR domain on the CAR T cell is able to directly kill the cells. Cytotoxicity against Her2-positive SKOV3 cells will occur when the CD19-anti-Her2 bridging protein binds to both the anti-CD19 CAR domain on the CAR T cells and to the target tumor cells, thereby forming a cytotoxic synapse. The components of the cytotoxicity assay were added in three ways: a) CAR-CD19 T cells, bridging protein and target cells were added together at same time, b) CAR-CD19 T cells were added to a premixture of bridging protein and target tumor cells, which had been pre-incubated at 37°C for 10 minutes, or c) the CAR-CD19 T cells were premixed with bridging protein and pre-incubated at 37°C for 10 minutes, and then added to target tumor cells. In all instances the bridging protein was added at 1 μg/ml, a concentration shown to be saturating for binding to CAR-CD19 T cells (see Supplemental Fig 2b). There was no difference in the degree of cytotoxicity observed among the three different conditions on either Nalm6 cells or SKOV3 cells (Fig 2c). These experiments

demonstrated that pre-binding of a CD19-anti-Her2 bridging protein does not negatively impact the ability of the CAR-CD19 T cells to directly or indirectly kill the target cells.

Next, CAR-CD19 T cell cytotoxicity curves were derived for killing Her-2 expressing SKOV3 and BT474 cells in the presence of the CD19-anti-Her2 bridging protein. The bridging proteins mediated very potent cytotoxicity with low pM IC_{50} values (Table 2, Fig 2d,e).

Figure 2. A CD19-anti-Her2 bridging protein mediates potent CAR-CD19 T cell cytotoxic activity *in vitro*. A) Phenotype of transduced and expanded CAR-CD19 T cells (donor 45): CAR-CD19 T cells were 54% CAR-positive by anti-Flag-tag staining. B) The CAR-CD19 T cells were tested for cytotoxicity against Nalm6 cells at different E:T ratios (10:1, blue; 3:1, teal; 1:1 light blue) and compared to donor-matched untransduced cells (UTD) at the same E:T ratios; all comparisons to UTD controls were significant. This assay is run routinely on all CAR-CD19-based CAR T cells; the extent of cytotoxicity varies among donors. C) Bridging protein, CAR-CD19 T cells (donor 54, 58% Flag-positive) and target tumor cells were added simultaneously (red bars) or bridging proteins and tumor cells were preincubated then added to CAR-T cells (light blue bars) or bridging proteins and CAR-T cells were preincubated then added to tumor cells (black bars). The E:T ratio used was 5:1. Controls were CAR-CD19 T cells, target cells plus bridging protein only ('BP') or target cells alone in culture ('none'). Nalm6 (left) and SKOV3 (right) cytotoxicity profiles are shown. The data are from duplicate wells; the experiment was performed twice with similar results. D,E) Dose response cytotoxicity curves using an E:T ratio of 10:1 CAR-CD19 T cells and target cells and varying the concentration of the CD19-anti-Her2 bridging protein or the control CD19-ECD. Target cell lines SKOV3 (D) and BT474 (E) are shown. The CAR-CD19 T cells used for the SKOV3 assay were from donor 54 (47% Flag-positive); donor 69 CAR-CD19 T cells (55% Flag-positive) were used for the BT474 assay. The data are from triplicate wells; the experiment was performed twice with similar results. All statistical tests were performed as 2-sided T tests. For Panels D and E, * indicates significance of $p < 0.0001$ and ** indicates significance of $p < 0.02$.

A dual-antigen-directed bridging protein potently targets Her2 and EGFR

Having successfully engineered the CD19-anti-Her2 bridging protein we added a second antigen-targeting domain that binds EGFR. The resulting bridging protein consists of anti-Her2 - CD19 ECD - anti-EGFR (#460, Table 1). A bridging protein targeting EGFR was also constructed (#416, Supplemental Table 1). Expression constructs were used to transfect 293T cells and the bridging proteins were purified. The binding affinities of single-antigen and the dual-antigen bridging proteins for the target antigens Her2 and EGFR were established using flow cytometric binding assays and Her2-positive, EGFR-positive or dual Her2/EGFR positive cell lines (Supplemental Figure 4). The dual-antigen targeting bridging protein #460 bound to the dual Her2/EGFR-positive cell line SKOV3 with an EC_{50} value of 2.5 nM which was similar to the affinity obtained on the single antigen cell lines K562-EGFR and BT474 and the affinity seen using the single antigen binding bridging proteins (Table 3, Supplemental Fig 5).

Next, the potency of the multi-antigen bridging protein in mediating CAR-CD19 T cell cytotoxicity against Her2-positive, EGFR-positive and dual-antigen-positive cell lines was determined and IC_{50} values were calculated. Dual antigen bridging protein-mediated cytotoxicity was highly effective against single antigen-positive cells, whether Her2-positive or EGFR-positive, with IC_{50} values ranging from 5 pM - 19 pM (Table 3, Supplemental Fig 6). Notably, the dual bridging protein was even more potent against dual-antigen positive cell lines, with an IC_{50} values of 1.4 pM for SKOV3 cells in the presence of anti-CD19 CAR T cells (Table 3, Supplemental Figure 6). The single antigen bridging proteins CD19 anti-Her2 and CD19-anti-EGFR was at least 10-fold less potent (Table 3, Supplemental Fig 6).

Table 3. Activity of a dual antigen targeting bridging protein. Data are presented as mean +/- standard error (if n ≥ 2). Top: Binding of single antigen and dual antigen bridging proteins to single and dual-antigen positive cell lines. Binding was detected with anti-CD19 antibody FMC63 staining and the EC_{50} values were derived from dose response flow cytometric analyses. Bottom: Bridging protein-mediated CAR-CD19 cytotoxicity against Her2-positive cell lines. CAR-CD19 T cells were used at an E:T ratio of 10:1. IC_{50} values were derived from a titration of the bridging protein concentration in the assays. A 0 indicates that binding or activity were not detectable above background levels; a '-' indicates that the experiment was not performed.

Bridging protein binding affinity in flow cytometry assays (EC_{50})				
cell line	antigens expressed	anti-Her2-CD19-anti-EGFR (#460)	CD19-anti-Her2 (#311)	CD19-anti-EGFR (#416)
BT474	Her2 only	2.5 nM n=1	3.8 +/- 1.1 nM n=2	-
K562-EGFR	EGFR only	0.6 nM n=1	0 n=2	0.52 nM n=1
SKOV3	Her2/EGFR	0.44 nM n=1	2.5 +/- 0.6 nM n=3	0.37 nM n=1
Bridging protein mediated cytotoxicity by CAR-CD19 T cells (IC_{50})				
cell line	antigens expressed	anti-Her2-CD19-anti-EGFR (#460)	CD19-anti-Her2 (#311)	CD19-anti-EGFR (#416)
BT474	Her2 only	5.1 pM n=1	24.4 +/- 3.7 pM n=4	0 n=2
K562-EGFR	EGFR only	19.1 pM	-	20.9 pM

		n=1		n=1
SKOV3	Her2/EGFR	1.4 pM n=1	11.7 pM n=1	13 pM n=1

CD19-bridging proteins do not bind the CD19-cis ligands CD21 and CD81

CD19 binds CD21 in cis and reportedly binds tetraspanins such as CD81 [21, 22]. We used a panel of cell lines expressing CD20 (Raji), CD21 (Raji), CD81 (Raji, SKOV3, K562), and Her2 (SKOV3), or none of these antigens (U937), to evaluate potential trans-binding of the CD19-anti-Her2 bridging protein. Binding to all four cell lines was evaluated by flow cytometry using an anti-His-tag antibody and the anti-CD19 antibody FMC63. As expected, the CD19 anti-Her2 bridging protein bound SKOV3 cells via the anti-Her2 scFv. The bridging protein did not bind to Raji cells (Her2-negative, CD21-positive, CD81-positive) as detected by anti-His-tag antibody staining (Supplemental Table S2). In order to rule out sequestration of CD21 and CD81 by endogenous CD19 in Raji cells we used OCI-LY3 cells (a lymphoma cell line) that do not express CD19. The bridging protein did not bind to OCI-LY3 (Supplemental Table S2). Representative flow cytometry data are presented (Supplemental Fig 7).

Detection of bridging protein with the anti-CD19 antibody FMC63 is possible for those cell lines which are CD19-negative: binding was observed with SKOV3 cells (Her2-positive, CD81-positive) but not with K562 cells (Her2-negative, CD81-positive) or U937 cells (negative for CD21, CD81 and Her2) (Supplemental Table S2, Supplemental Fig 7). We previously showed that CAR-CD19 T cells do not kill SKOV3 cells via CD81 binding in the presence of the

CD19-ECD control protein, but only in the presence of the CD19-anti-Her2 bridging protein [18]. These results show that the CD19 ECD cannot interact with either CD21 or CD81.

Bridging protein secretion by CAR-CD19 T cells

To generate CAR-CD19 cells that secrete bridging proteins we cloned CD19-anti-Her2 sequences into a lentiviral vector downstream of a CAR-CD19 sequence and a P2A site to create a Her2-bridging CAR-CD19 (#374, Table 1). Viral particles were produced with a transducing titer of 1.8 x 2.5 x 10^9 TU/ml. T cells isolated from human donors were transduced with the lentiviral particles and analyzed for expression of the CAR-CD19 domain by flow cytometry. Using 6 different donors, we determined that the mean expression of the CAR-CD19 domain on the transduced primary T cells was 43% (range 24% - 63%, SD = 13%). Bridging protein secretion was measured by ELISA (FMC63 capture and anti-His detection). The mean secretion of the bridging protein was 40.2 ng/ml (n=7 donors, duplicate points, range 10-81 ng/ml) in activated CAR T cell culture supernatants.

Her2-bridging CAR-CD19 T cells have potent activity *in vitro*

Her2-bridging CAR-CD19 T cells were generated using normal human T cells (donor 45). The lentiviral transduction produced 47% CAR-positive T cells and the T cell pool was 38.5% CD8-positive and 99.5% CD3-positive (Fig 3a). The secretion of bridging protein was measured at 24 ng/ml in the activation assay (Fig 3b). Her2-bridging CAR-CD19 T cells were tested in cytotoxicity assays using either CD19-positive Nalm6 cells or Her2-positive SKOV3 cells at different E:T ratios; UTD T cells were used as a negative control. E:T ratios were calculated using the total T cell number and were not adjusted to reflect %-CAR positive cells. CD19-positive Nalm6 cells were potently killed by Her2-bridging CAR-CD19 T cells, showing that the

bridging protein did not interfere with CD19 recognition by the CAR-CD19 domain (Fig 3b). Her2-positive SKOV3 cells were also potently killed by Her2-bridging CAR-CD19 T cells, demonstrating that the secretion of the bridging protein was sufficient to retarget the CAR-CD19 domain to SKOV3 cells. Potent cytotoxicity was seen down to an E:T ratio of 1:1 (Fig 3c).

These results show that Her2-bridging CAR-CD19 T cells can efficiently kill Her2-positive target cells. This is the first demonstration of cytotoxic elimination of CD19-negative tumor cells by retargeted CAR-CD19 T cells.

Figure 3. Her2-bridging CAR-CD19 T cells are cytotoxic against both CD19-positive and Her2-positive cells *in vitro*. (A,B) Example of the flow cytometry gating strategy (A) and the ELISA assay used (B) to determine the purity and phenotype of transduced human donor CAR-CD19 T cells that secrete a bridging protein. C) Her2-bridging CAR-CD19 T cells were added at different E:T ratios to Nalm6 cells (left) or SKOV3 cells (right) and cytotoxicity was measured. E:T ratios used were 10:1 (red bars), 3:1 (light blue bars) and 1:1 (black bars). The donor matched UTD cells are also shown at each E:T ratio.

Restimulation Assay

Successful repetitive CAR T cell stimulation *in vitro* predicts potent CAR T cell activity *in vivo* [23], as repetitive stimulation models the waves of functional activity and cell proliferation needed for serial cytotoxicity. We investigated the impact of serial restimulation on Her2-bridging CAR-CD19 T cells using either Raji cells (CD19-positive lymphoma) or SKOV3 cells (Her2-positive ovarian carcinoma) or both, to model *in vitro* the potential encounters that the CAR T cell population would undergo in the patient setting *in vivo*.

One variable that complicates analysis of the re-stimulation assay results is the differential proliferative capacity of target cells during the course of the *in vitro* cell culture based cytotoxicity assay. Suspension-cultured B cell lines undergo rapid proliferation whereas attachment-cultured SKOV3 cells divide much more slowly and become contact-inhibited once confluent. In order to control for potential differential target cell proliferation in the assay we used mitomycin-c treatment to stop cell proliferation. Mitomycin-c is a double-stranded DNA alkylating agent that covalently crosslinks DNA, inhibiting DNA synthesis and cell proliferation. The cells treated were CD19-positive Raji lymphoma cells and Her2-positive SKOV3 ovarian carcinoma cells and the doses used were sublethal for at least 48 hours [24, 25].

Target tumor cells were treated with mitomycin-c, washed extensively, then cultured with CAR T cells for 48 hours. The CAR T cells were then washed and rested in media for 48 hours before being restimulated with a new preparation of mitomycin-c treated target cells. The process of stimulation, rest and restimulation was repeated through 4 cycles, through day 15. Her2-bridging CAR-CD19 T cells were stimulated repeatedly with either Raji cells or with SKOV3 cells. Her2-bridging CAR-CD19 T cells proliferated robustly in response to Raji cell restimulation through 4 rounds, as did CAR-CD19 T cells (Figure 4a). In contrast, Her2-bridging CAR-CD19 T cells did not increase dramatically above day 0 cell numbers when restimulated with SKOV3 cells, nor did CAR-Her2 T cells (Figure 4a). The differences in increase of CAR-CD19 T cells or Her2-bridging CAR-CD19 T cells in response to Raji cell restimulation versus no stimulation or SKOV3 restimulation were highly significant ($p < 0.001$, t-test for two independent samples for each comparison, n=3). The cells restimulated with SKOV3 cells were viable, and they retained some cytotoxic activity through 3 rounds of stimulation (see below).

The Her2-bridging CAR-CD19 T cells recovered from each round retained cytotoxic activity (Fig 3b). In each cytotoxicity experiment the same number of CD3-positive CAR T cells were presented to luciferase-labeled target cells at a 5:1 E:T ratio. Representative results show that continual restimulation by Raji cells allows the Her2-bridging CAR-CD19 T cell population to maintain very high cytotoxic activity against both JeKo-1 cells (a B lymphoma cell line) and SKOV3 cells (Fig 4b). After 1 stimulation and after 3 stimulations, cytotoxic activity was sufficient to kill >95% of the target cells. In contrast, continual restimulation by SKOV3 cells gradually impacted the ability of the CAR T cells to mediate full cytotoxic activity. After 1 stimulation, Her2-bridging CAR-CD19 T cells were able to kill 100% of target tumor cells, whether JeKo-1 B cells or SKOV3 ovarian carcinoma cells (Fig 4b). After 3 rounds of SKOV3 cell stimulation, Her2-bridging CAR-CD19 T cells lost approximately 80% of cytotoxic activity (Fig 4b). Similar results were seen with the control CAR-CD19 T cells and the control CAR-Her2 T cells, ie. diminished cytotoxic capacity was only seen when T cells were restimulated by SKOV3 cells (Fig 4b). The difference in cytotoxic activity of CAR-374 cells when stimulated with Raji cells versus SKOV3 cells was significant at Round 3 whether the target cell was JeKo-1 or SKOV3 ($p < 0.001$, t-test for two independent samples for each comparison, n=3).

Figure 4. CAR T cell activity in response to restimulation. A) Extent of CAR T cell proliferation after 2 rounds and 4 rounds of Raji cell stimulation, SKOV3 cell restimulation or no stimulation; CAR T cell types are indicated below the x-axis. B) Extent of CAR T cell-mediated cytotoxicity against target tumor cells and 1 round and 3 rounds of Raji cell stimulation, SKOV3 cell restimulation or no stimulation. The round of stimulation, cell source of stimulation is indicated, and target cell in the cytotoxicity assay are indicated. * = p , 0.001. NS = no significant differences.

Bridging protein-secreting CAR-CD19 T cells are cytotoxic *in vivo*

Having established that Her2-bridging CAR19 T cells have cytotoxic activity against CD19-positive Nalm6 cells and Her2-positive SKOV3 cells *in vitro*, we tested the activity of these cells *in vivo*. Studies have been performed with anti-CD19 CAR T cells that secrete slightly different forms of the bridging protein (#142, Supplemental Table 1 and #374, Table 1), with little apparent difference in outcomes. First, we analyzed the circulating half-life of purified bridging protein (#42) by injecting immunodeficient mice IV or i.p. with 200 μg of protein and analyzing protein concentration in the serum. The $T_{1/2}$ was determined to be ~1 hour after IV or i.p. adminstration (63 minutes and 65 minutes, respectively, S8 Fig). The short half-life was expected given the small size of the bridging protein and the absence of any half-life extension technology such as an Fc-domain, a PEG-domain or an anti-albumin binding domain. The half-life of the modified form of the bridging protein (#340) is not expected to be significantly different because no half-life extension technology (Fc domain or anti-albumin binder) was added.

We tested the activity of the CAR-CD19 and Her2-bridging CAR-CD19 T cells using xenografts in NOD-SCID-gamma common chain-deficient (NSG) mice. NSG mice injected iv with the CD19-positive cell line Nalm6 develop disseminated leukemia which is lethal approximately three weeks after injection. CAR-CD19 T cells effectively eliminated the *in vivo* growth and dissemination of Nalm6 cells as expected (S9 Fig).

To evaluate Her2-bridging CAR-CD19 T cells we injected 1 x 10^6 Nalm6-luciferase cells on day 1 and allowed the leukemic cells to expand for 4 days. The baseline degree of

luminescence was established, mice were placed randomly into cohorts, and 3 different doses of CAR-T cells were injected iv. Mice were imaged weekly to determine the extent of disease burden. A dose response was observed for Her2-bridging CAR-CD19 T cells T cells with full eradication observed at the higher doses (Fig 5a). The treatment groups are also shown separately from the control groups in order to enhance visualization of the dose response (Fig 5b). This study demonstrates that Her2-bridging CAR-CD19 T cells recognize and eliminate CD19-positive cells *in vivo.*

Next we extended the *in vivo* modeling to the Her2-positive tumor cell line SKOV3. SKOV3 cells (1 x 10^6) were implanted subcutaneously and allowed to establish. Mice were then randomized, the baseline degree of luminescence was established, and 1 x 10^7 CAR T cells were injected iv on day 14, at which time the tumors averaged 150mm^3 by caliper measurement. CAR-CD19 T cells (CAR-254) and Her2-bridging CAR-CD19 T cells were evaluated in this model. Mice were imaged weekly and caliper measurements of the tumor were taken twice weekly. By day 14 post CAR T cell injection the cohorts that received the Her2-bridging CAR-CD19 T cells had cleared the tumor mass as measured by caliper (Fig 5c). Tumor growth was significantly less than that measured in the negative-control cohorts (CAR-CD19 injected mice, or untreated mice (NA), Fig 5c). In a second study the *in vivo* activity of Her2-bridging CAR-CD19 T cells and CAR-Her2 T cells (CAR-390, Table 1) was compared and we found that the tumor control curves and the survival curves were indistinguishable (Fig 5 d,e). All mice treated with Her2-bridging CAR19 T cells and CAR-Her2 T cells survived to day 42, while all animals in the negative control groups had to be sacrificed due to tumor burden.

Figure 5. Her2-bridging CAR-CD19 T cells are efficacious *in vivo*. A) Dose responsive elimination of pre-established leukemia in an NSG mouse model was monitored after Her2-bridging CAR-CD19 T cells (CAR-142 and CAR-374, donor 36, 99.8% CD3-positive, 67% CD8-positivem, 59% Flag-tag-positive) were administered at doses ranging from 2 x 10^6 to 1 x 10^7 cells/mouse. Luminescence values for all cohorts (A) and the treatment cohorts (B) are shown. C-E) CAR T cells (donor 45, 99.2% CD3-positive, 41% CD8-positive, 38% Flag-tag-positive) were evaluated in a SKOV3 ovarian carcinoma model in NSG mice. C) CAR-142 T cells controlled SKOV3 tumor growth while control CAR T cells (CAR-254) had no effect. D) CAR-142 T cell control of SKOV3 tumor growth as compared to CAR-Her2 (CAR-390). CAR-142 and CAR-390 fully controlled tumor growth, while control mice succumbed and had to be euthanized by day 42 (panel E). * = $p < 0.001$. ** = $p < 0.05$. NS = no significant differences.

In a followup study, serial rechallenge was evaluated. Her2-bridging CAR19 T cells were injected as described above and tumor growth was evaluated through day 42 (Fig 6a). All animals in the negative control groups (n=30) had to be euthanized due to tumor burden; in contrast only one animal was lost in the Her2-bridging CAR19 T cell treated cohort (Fig 6b). The surviving animals in the Her2-bridging CAR19 T cell treated cohort were rested until day 55 (post tumor challenge) and then 4 mice were rechallenged with 1 x 10^6 Nalm6 cells to investigate whether the remaining CAR T cell pool could react to directly presented CD19 antigen. Three naïve NSG mice were also injected as a positive control for tumor engraftment and growth. The mice that had initially cleared the SKOV3 tumor effectively eliminated the Nalm6 cells, and there was no Nalm6 engraftment or expansion (Fig 6c). In contrast the naïve mice challenged with Nalm6 cells rapidly developed disseminated leukemia (Fig 6c) and were sacrificed by day 21 due to tumor burden.

Figure 6. Her2-bridging CAR-CD19 T cells eliminate Her2-positive tumors and CD19-positive tumors in a serial challenge *in vivo* model. A-C) CAR T cells (donor 45, 99.2% CD3-positive, 45% CD8-positive, 34% Flag-tag-positive) were evaluated in a SKOV3 ovarian carcinoma model in NSG mice. A) CAR-374 treatment eliminated preestablished SKOV3 tumors in the NSG mouse model. B) 90% of CAR-374 treated mice survived past day 36, by which point the control mice were beginning to require euthanasia. C) CAR-374 that survived the SKOV3 challenge subsequently cleared CD19-positive Nalm6 leukemia challenge; all individual mice are shown. * = $p < 0.001$.

These studies demonstrated that both mechanisms inherent to Her2-bridging CAR-CD19 T cells were active *in vivo*: the T cells could eliminate CD19-positive Nalm6 cells directly via the CAR-CD19 domain and also indirectly, via recognition of the CD19 ECD on the bridging protein that bound to the Her2-positive tumor cells.

Discussion

Here we describe a novel approach to CAR-T cell therapy with three unique attributes: first, we demonstrate that it is possible to retarget CAR-CD19 T cells to kill any solid or hematologic tumor cell, exemplified here using Her2-positive solid tumor cells; second, we encode the CAR-CD19 domain and the CD19-bridging protein together within a lentiviral vector, such that it is secreted in parallel with expression of the CAR on the transduced T cell surface, thereby leveraging the inherent advantages of CAR-CD19 T cells; and third, we use modular CD19-bridging proteins, which apply well understood protein-engineering principles and solutions to multiple limitations facing the CAR-T cell field, including providing a platform for multi-antigen targeting.

Robust *in vivo* expansion followed by prolonged CAR-T cell persistence is critical for the efficacy of CAR-T cell therapy directed to the B cell tumor antigen CD19 for the treatment of hematological malignancies [26-28]. In contrast, most solid tumor-targeted CAR-T cells appear to have poor persistence properties, irrespective of the antigen targeted. For example, in a phase 1 clinical study of CAR T cell therapy for biliary tract and pancreatic cancers, Her2-targeting CAR-T cells showed peak expansion of 7-fold or less above baseline at day 9 post-injection, dropping thereafter [29]. Similarly, CAR-T cells targeting EGFRvIII that were administered for the treatment of glioblastoma persisted 21 days or less after infusion and had minimal clinical impact [30, 31]. A CAR-T cell therapy targeting IL13Rα2 reported sustained clinical impact in one patient despite minimal CAR cell persistence, and there were no other notable responses in that trial [32]. Notably, CAR T cells targeting PSMA expanded up to 500-fold over baseline following administration of 10^9 – 10^{10} total T cells to patients [33]. Expansion in patients appeared to be Il-2-dependent and lasted up to 4 weeks; several partial clinical responses were noted, but the duration of response was not reported. In general, poor CAR T persistence in solid tumors is associated with minimal clinical efficacy. Several interesting efforts to incorporate CARs into T cells that recognize viral antigens as a means of enhancing persistence have been advanced including a preclinical study using EBV-specific cytotoxic T cells to express an anti-CD30 CAR domain, and a clinical study utilizing HBV-specific T cells to express an anti-Her2 CAR domain [34, 35]. These therapeutics continue to advance in the clinic and it will be of keen interest to evaluate the expansion and persistence characteristics of these virus-specific T cells in patients.

Advances in the field focused on improving CAR-T cell activity include providing cytokine or chemokine support, preventing immunosuppression, and targeting intrinsic pathways to improve CAR-T cell fitness and persistence [36-39]. Recent efforts to provide artificial and immunologically favorable antigen presentation to CAR T cells also aim to improve CAR T cell fitness and persistence. For example an exogenously added CAR-T ligand was developed that binds to albumin, traffics to lymph nodes and is displayed by antigen-presenting cells (APC) [40]. CAR-T cells that encounter this ligand in the lymph node are therefore stimulated not only by the displayed antigen but also by costimulatory receptors and cytokines produced by the APCs. In another example, *in vivo* administration of a nanoparticulate RNA vaccine was used to deliver a CAR antigen into lymphoid compartments in order to stimulate adoptively transferred CAR-T cells. Again, presentation of the target antigen on APCs promotes immunologically productive activation and expansion of the injected CAR-T cells [41]. Notably, engagement of relevant stimulatory, chemokine and adhesion signals appears to favor the development of T cell memory [42], a critical element in long term immune protection. Finally, the importance of immunologically relevant T cell activation has been demonstrated in the immune checkpoint field, with defined roles for organized secondary and tertiary lymphoid organs becoming apparent [43-46].

In our system the CAR-CD19 T cell interaction with normal B cells will support production of immunologically relevant stimulatory signals including adhesion interactions, chemokine and cytokine signals, and costimulatory signals [47-50]. This organic presentation of immunologically relevant antigen does not require administration of additional agents or exogenous antigen, since B cells are APCs and represent a self-renewing source of CD19 that are

present in lymphoid organs and in circulation. Moreover, in the *in vitro* experimental setting we showed that interaction of the Her-2 bridging CAR-CD19 T cells with a B cell target cell (Raji cells) had a distinctly different outcome than interaction with a solid tumor cell target (SKOV3), suggesting that at least some T cell supportive signals are present even if the target B cell is malignant. In the *in vivo* model, serial presentation of antigens (Her2, CD19) showed that the Her2-bridging CAR-CD19 T cells could engage both cell types.

Even in the setting of B cell leukemias and lymphomas, expression of CD19 on normal B cells may be critical for prolonged persistence of CAR T cells. In fully murine (syngeneic) models of CAR-CD19 therapy of B cell malignancy, control of tumor cell outgrowth over time and in the context of leukemic rechallenge required the presence of normal B cells [51, 52]. This observation suggests a unique role for normal B cells in providing a non-tumor dependent, self-renewing antigen source to support CAR-CD19 persistence. This concept is clinically validated, since some CAR-CD19-treated patients who have relapsed with CD19-negative tumors have persistent CAR-CD19 T cells in their circulation and continued B cell aplasia, demonstrating that the CAR-CD19 T cells remain functional [53]. An analysis of CAR-CD19 treatment of B cell leukemias found that the primary driver of CAR-CD19 T cell expansion and durable functional persistence was a cumulative burden of >15% of CD19 expressing leukemic and normal B cells in the bone marrow prior to lymphodepletion, and furthermore, that neither CAR T cell dose nor leukemia burden alone could predict CAR-CD19 T cell expansion and duration of engraftment [14, 54]. These results strongly suggest a critical role for normal CD19-positive B cells in supporting CAR-CD19 T cell expansion and persistence. In the setting of CAR-CD19 T cells secreting bridging proteins, CD19 expressed on normal B cells will be a readily accessed antigen

source, to allow immunologically relevant CAR T cell expansion and to enhance persistence regardless of the targeted tumor antigen and indication.

B cell aplasia may be an important complication in some patients, however in the majority of patients, including most adults, B cell aplasia is a manageable toxicity. Hematology oncologists and rheumatologists have worked with B cell depletion agents for many years and the protocols for managing B cell aplasia are well understood [55-57]. It is conceivable that targeting B cells in the manner described will induce clinical toxicity such as cytokine release syndrome; such toxicities related to CAR T cell activity have also become increasing manageable [58, 59]. Finally, encouraging preclinical demonstration of the utility of off-the shelf agents such as dasatinib may lead to control over CAR T cell activity in the clinical setting [12, 60, 61].

The phenomenon of tumor antigen loss in response to CAR-T cell therapy is observed across indications and antigens and represents another major issue confronting adoptive cell therapy. The findings to date include the loss of target antigens from the cell surface in hematologic malignancies including ALL, NHL and multiple myeloma, and rapid tumor cell population escape due to the heterogeneity of antigen expression in solid tumors [62-64]. It is clear that countering resistance due to antigen loss and tumor antigen heterogeneity will require multi-antigen targeting solutions in many different cancer indications. Our use of CD19-bridging proteins provides a simple and pragmatic solution to this problem since CD19-bridging proteins can be readily produced in single-antigen, dual-antigen and multi-antigen targeting formats. As shown herein, a bi-specific CD19-bridging protein containing an anti-Her2 and an anti-EGFR scFv killed tumor cell expressing one or the other antigen, while showing exceptional potency when both antigens were present. We have used VHH domains in many of our constructs, and

the linkage of two, three or more VHHs in series is well-established [65]. Thus, rapid, flexible and modular extension to three or more antigens is readily achievable with the CD19-bridging protein format, which builds on decades of established antibody and antibody fragment-based solutions [65, 66].

The adaptor CAR T cell field, in which antibodies, Fabs or other biologic constructs are used to link universal CARs to tumor antigens is an adjacent technology solution. Examples include CARs that target Fc receptors, peptides, haptens and leucine zipper binding [67]. The singular issue with such technologies is their reliance on tumor antigen expression, thus if the target antigen is lost the adaptor won't bind and the CAR cannot recognize the tumor cell. It is possible to create multiple adaptors to different antigens and use these in series or simultaneously, although regulatory and clinical translation may be slow.

There are alternative elegant solutions to dual antigen targeting, including tandem CARs, dual CARs, switch-gated CARs [68-70]; these are created via manipulation of the encoded CAR domain sequence, which then must be successfully expressed on the T cell surface. As such technologies are extended to solid tumor antigens the expression of antigen on normal tissues will become a concern (see below), and may necessitate tuning of CAR affinities. Extension to three or more antigens while still retaining tumor targeting selectivity will require precise engineering. For example a recent paper described the use of defined ankyrin repeat domains (DARPins) to target three antigens successfully [71]. The technology was limited however as the potency of the trispecific CAR was lower than the corresponding monospecific CARs against tumor cells expressing a single target, revealing a potential limitation of multi-specific designs when expressed on the CAR T cell surface. Further, the issue of normal tissue cytotoxicity (eg. on EGFR) was not addressed. Thus the elegance of multi-CAR technologies is balanced by the

difficulty, to date, of successfully engineering and expressing optimal constructs. In contrast, secretion or cell surface expression of proteins concurrent with CAR expression in CAR-CD19 T cells is well-established. This includes cytokines, receptors, and antibody domains, among others [37, 72]. Further, BiTE protein secretion from activated T cells or CAR-T cells does not activate, anergize or exhaust the T cells despite the fact that these proteins bind back to T cells via their anti-CD3 component [73]. For example, an anti-CD3 x anti-EGFR BiTE was successfully secreted from an EGFRvIII-directed CAR-T cell showing that such secretion does not interfere with T cell function [8]. Further, both EGFR and EGFRvIII were specifically targeted in this system, demonstrating the utility of multi-antigen targeting from a single CAR T cell. In our system the secreted bridging protein likewise does not bind back to the CAR T cell in a manner that interferes with T cell function, and similarly enables multi-antigen targeting. The result is potent retargeted killing of the CD19-negative target cells with retention of cytotoxicity against CD19-positive cells.

Indeed, BiTEs and other forms of T cell engagers represent another adjacent technology solution, with many formats targeting diverse antigens under development. The major differentiation between the BiTE-like technologies and the CAR T engagers as described herein is specificity for the T cell. T cell engagers can bind to various anti-CD3-positive T cell subsets, to uncertain effect. Furthermore, several reviews have stressed the impotance of antigen-experienced T cell subsets in mediating T cell engager activity, posing a challenge in settings where such antigen-experienced cells are rare [73, 74]. In contrast the bridging proteins, as CAR T cell engagers, only bind to and activate the engineered cytotoxic CAR T cell, which we believe will be in sufficient concentration due to expansion from normal B cell engagement as well as

antigen engagement via the bridging protein. Regardless, advances in the T cell and NK cell engager fields are interesting and will likely yield broader clinical application [75].

Our approach offers additional advantages. As a discrete entity, the secreted bridging protein has no obvious liabilities. The half-life is very short, which will limit systemic exposure and binding to normal tissues via the antigen-binding domains. Further, there is no Fc-domain that might mediate immune activation. The CD19 ECD is also essentially inert, having low potential immunogenicity [18] and no detectable binding to target cells expressing CD21 and/or CD81 that normally function, in cis, to mediate CD19 signaling within the B cell receptor complex. Finally, no detectable CAR-CD19-dependent killing can be seen in the presence of CD19 ECD alone [18]. We conclude that as a discrete entity, a bridging protein is functionally inert and has limited systemic exposure. Thus secreted bridging proteins should be biased to accumulate only where cell and antigen density is most abundant, ie. in the tumor itself, and should therefore primarily mediate activation of a CAR-CD19 T cell when bridging to an antigen-positive tumor cell. Such a system should provide a superior therapeutic index when compared to antigen-targeting CAR T cells.

One compelling translational strategy we are pursuing is to target Her2-positive CNS metastases in breast cancer, a leading cause of therapy failure. Systemically injected Her2-bridging CAR-CD19 T cells will expand in the presence of normal B cells, even if a patient remains on anti-Her2 antibody therapy (eg. trastuzumab plus pertuzumab). Our ability to allow the patient to remain on standard of care therapy has two important consequences: 1) they are less likely to experience systemic tumor progression due to treatment interruption, and 2) the presence of trastuzumab will block systemically expressed Her2, making it less likely for the bridging protein to bind to any normal tissues expressing Her2. Of note, the antibody

therapeutics used in Her2-positive cancer therapy (trastuzumab plus pertuzumab, or ADCs) cannot cross the blood-brain barrier effectively, and will not bind to Her2 in the CNS. In contrast, activated CAR-CD19 T cells readily access the CNS where they can find and control cancers [76, 77]. In the CNS the only Her2 present will be on the metastases, as normal brain and neuronal tissues are Her2-negative. Finally we note a recent paper showing that local activity of CAR-Her2 T cells in the presence of abundant tumor antigen did not cause systemic toxicity. In this singular case report, locally abundant rhabdomyosarcoma cells in the bone marrow supported CAR T expansion (following multiple CAR infusions) and 6 months of tumor control. Importantly, on-target/off-tumor toxicity was not reported [78]. This suggests that local accumulation of CAR T cells at the site of the tumor (here, in the bone marrow) improves the therapeutic index by limiting systemic exposure. These results are encouraging in the context of treating Her2-positive CNS metastases, as described above.

In summary, we present a universal method to retarget CAR-CD19 T cells to hematologic or solid tumor antigens, using CD19-bridging proteins secreted by the CAR-CD19 itself. This approach retains all the advantages of CAR-CD19 T cells, including optimal fitness and persistence and well a developed manufacturing history. In addition, the focus on protein engineering to create flexible and modular CD19-bridging proteins provides simple solutions to potency, antigen selectivity, and multi-antigen targeting.

Materials and Methods

Human cell lines

SKOV3-luciferase (Cell Biolabs, San Diego, CA) were grown in RPMI containing 10% FBS and 0.8 mg/ml neomycin. BT474, Nalm6, K562, U937, Jeko-1, and 293T cells (ATCC, Manassas, VA) Raji cells (MilliporeSigma, St. Louis, MO), and 293FT cells (Thermo Fisher, Waltham, MA) were cultured according to supplier specifications. OCI-LY3 were cultured according to the suppliers instructions (DSMZ, Braunschweig, Germany). Stable cell lines expressing firefly luciferase were generated using lentiviral particle transduction and puromycin selection (GeneCopoeia, Rockville, MD).

Protein expression constructs

Genes were chemically synthesized by GenScript (Piscataway, NJ) and assembled into pcDNA3.1+ vectors (Invitrogen, Carlsbad, CA). The native CD19 ECD constructs were made with amino acids 1 to 278 (UniProtKB accession number P15391); eg. control construct #28. Construct #117 was made using the CD22 ECD amino acids 20-332 (UniProtKB accession number P20273 with a N101A mutation) and the anti-Her2 scFv sequence derived from trastuzumab [79]. Constructs #311 and #340 were made with stabilized CD19 ECD and the humanized anti-Her2 scFv (human 4D5 scFv, VH-G4Sx3-VL) [18]. These constructs are expressed at higher concentration than a previously decribed forms that contained the wildtype CD19 ECD (eg. as in #42) [18]. Construct #416 was made using a stabilized CD19 ECD and an anti-EGFR scFv sequence derived from panitumumab VH and VL sequences (Genbank accession numbers LY588610 and LY588596, respectively). Construct #460 contains the trastuzumab scFv the C terminal stabilized CD19 ECD-A, a second G4S linker, the panitumumab anti-EGFR scFv. It was produced by ligation of the pantitumumab fragment into a

vector containing the trastuzumab-CD19 fusion. Constructs contained G4S linkers between functional domains and C-terminal 6xHis tags.

K562-EGFR generation

K562 cells expressing luciferase were transfected with a plasmid containing full-length EGFR (#OHu25437D, GenScript) using lipofectamine 2000 according to the manufacturer's protocol (Invitrogen). The cells were selected in G418 and clones isolated using limiting dilution.

Expression of the bridging proteins

293T cells were transfected with expression constructs using lipofectamine 2000 following the manufacturer's protocol (Invitrogen, Waltham, MA). On day 3 post transfection the cell culture supernatants were harvested via centrifugation at 12,000 RPM for 4 minutes at 4ºC. His tagged bridging proteins were purified from the 293T transfected cell supernatant using a Ni Sepharose HisTrap excel column following the manufacturer's protocol (GE Healthcare, Marlborough, MA). The relevant fractions were pooled and buffer exchanged to PBS.

CAR constructs

Construct #254 contains the FMC63 anti-CD19 CAR sequence (CAR-CD19). The anti-CD19 scFv sequence was derived from the FMC63 antibody [80], cloned in the VL-VH orientation, and includes a FLAG-tag, CD28 linker, transmembrane domain and cytoplasmic signaling domain (amino acids 114-220, UniProtKB accession number P10747) plus 4-1BB (amino acids

214-255, UniProtKB accession number Q07011) and CD3ζ (amino acids 52-164, UniProtKB accession number P20963) cytoplasmic signaling domains. The sequence was chemically synthesized (GenScript) and cloned into a derivative of the lentiviral vector, pCDH-CMV-MCS-EF1-Neo (Systems Biosciences, Palo Alto, CA) that contains an MSCV promoter. The CAR-CD19 sequence was also synthesized by Lentigen and cloned into their MSCV-contianing vector. Construct #390 (CAR-Her2) contains an scFv (Vh-Vl) from the anti-Her2 antibody FRP5 (GenBank accession number A22469) followed by the same components as the CAR-254 sequence (CAR-CD19: Flag tag, CD28 stalk transmembrane and cytoplasmic signaling domain and the 4-1BB and CD3ζ cytoplasmic signaling domains). The scFv portion of the CAR was chemically synthesized (Integrated DNA Technologies, Coralville, IA) and then assembled with a PCR fragment from the CAR-2 vector, minus the anti-CD19 scFv, using the NEBuilder Hi Fi DNA Assembly Master Mix (New England Biolabs, Beverly, MA). For the production of lentiviral particles, packaging plasmids pALD-VSVG-A, pALD-GagPol-A and pALD-Rev-A (Aldevron, Fargo, ND) and the expression plasmid were combined in Opti-MEM (Invitrogen). Trans-IT transfection reagent (Mirus, Madison, WI) was added. After incubation, the DNA/Trans-IT mixture was added to 293FT cells in Opti-MEM. After 24 hours, the media replaced with DMEM plus 10% FBS daily for 3 days and stored at 4ºC. The viral particles were precipitated by adding 5X PEG-IT (Systems Biosciences) incubating at 4ºC for 72 hours. The mixture was centrifuged at 3000 RCF for 30 minutes, the residual supernatant removed and the pellet resuspended in 200 µl PBS and stored at -80ºC.

CAR-CD19 constructs containing bridging proteins

Expression cassettes for use in lentiviral constructs were chemically synthesized and cloned into a lentivirus vector containing an MSCV promoter (Lentigen Technology, Gaithersburg, MD). All constructs expressing bridging proteins contained the CAR-CD19 sequence described for CAR-254, a P2A cleavage site, and then the bridging protein sequences. Construct #374 contains the bridging protein sequence from construct #340. As such this bridging protein contains a stabilized CD19 ECD and replaced an earlier construct that used the wildtype CD19 ECD (#142); the activity of the two Her2-bridging CARs was very similar. Lentiviral particles were produced at Lentigen.

CAR-T cell generation

For production and characterization of CAR T cells, CD3-positive human primary T cells were isolated from PBMC derived from normal human donors (Research Blood Components, Watertown, MA) and cultivated in ImmunoCult-XF T cell expansion medium (serum/xeno-free) supplemented with 50 IU/ml IL-2 at a density of 3 x 10^6 cells/mL, activated with CD3/CD28 T cell Activator reagent (STEMCELL Technologies, Vancouver, Canada) and transduced on day 1 with the CAR lentiviral particles in the presence of 1X Transdux (Systems Biosciences). Cells were propagated until harvest on day 10. Post-expansion, CAR T cells were stained with FLAG antibody to measure CAR expression. Briefly, 1 x 10^5 cells were incubated with anti-FLAG antibody (Thermo Fisher), diluted 1:100 in PBS for 60 minutes at 10°C, followed by a 1:100 dilution of anti-rabbit APC-conjugated antibody (Thermo Fisher). CAR T cells were stained for CD8 using anti-CD8 MEM-31 antibody, diluted 1:100 (Thermo Fisher). Cells were resuspended

in PBS and fixed at a final concentration of 2% paraformaldehyde. Cell populations were analyzed using an Accuri C6 flow cytometer (BD Biosciences, Franklin Lakes, NJ).

Analysis of bridging protein binding, specificity and affinity by ELISA

Plates were coated overnight at 4°C with 1.0 µg/mL anti-CD19 antibody FMC63 (#NBP2-52716, Novus Biologics, Centennial, CO) or 1.0 µg/mL purified Her2-Fc (#HE2-H5253, AcroBiosytems, Newark, DE), in 0.1 M carbonate, pH 9.5. The plate was blocked with 0.3% non-fat milk in TBS for 1 hour at room temperature. After washing in TBST 3 times, the bridging protein was titrated from a starting concentration of 5 µg/mL using serial 3-fold dilutions in TBS/1% BSA and incubated 1 hour at room temperature. Detection with Her2-Fc, biotinylated Her2 (#He2-H822R, AcroBiosystems), or antibody FMC63 was performed by adding the detection reagent at 1.0 µg/mL and incubating for 1 hour at room temperature. The plates were then washed 3 times, followed by a 1 hour incubation with a 1:2000 dilution of anti-human IgG-HRP (#109-035-088, Jackson ImmunoResearch, West Grove, PA) for Her2-Fc detection, HRP-steptavidin (#21130, Thermo Fisher) for biotinylated Her2 detection, and anti-mouse IgG-HRP (#115-035-062, Jackson ImmunoResearch) for FMC63 detection. Then, 1-Step Ultra TMB-ELISA solution (#34028, Thermo Fisher) was added to develop the peroxidase signal, and the plate was read at 405 nm. Curves were fit using a four parameter logistic regression to calculate the EC_{50}.

Flow cytometric analyses of bridging protein binding to cells and of cell surface antigen expression

When necessary, cells to be analyzed were detached with 0.5 mM EDTA in PBS. Tumor cells or lymphocytes were washed and analyzed in ice cold FACS buffer (PBS/1 % BSA/0.1% sodium azide). Cells were resuspended (5 x 10^5/100 µl) and purified bridging proteins (up to 10 µg/ml), or supernatants (100 µl) were added to 100 µl final volume and incubated with the cells at 4°C for 30 minutes. After washing, cells were resuspended (5 x 10^5/100 µl) and incubated with detection antibody at 4°C for 30 minutes. The cells were resuspended in 100 µl total volume and stained with 5 µl anti-His-PE (#IC050P, R&D Systems, Minneapolis, MN) or anti-CD19 antibody FMC63-PE (#MAB1794, MilliporeSigma, Burlington, MA) for 30 minutes at 4ºC , washed and resuspended using PBS, fixed with 1% paraformadehyde in PBS, and analyzed on the Accuri Flow Cytometer (BD Biosciences). Analysis of antigen expression by tumor cells was performed using flurochrome-conjugated monoclonal antibodies specific for the target antigen. Analysis of CAR T cell CD3 and CD8 expression was performed using PE-conjugated or APC-conjugated monoclonal antibodies specific for the target antigen.

Analysis of secreted bridging protein concentration

To measure the secretion of bridging protein by CAR T cells, 600,000 cells were added at $3x10^6$ cells/ml to a 96-well U-bottom plate. Cells were activated with 1X ImmunoCult Human CD3/CD28 T Cell Activator (#10971, Stemcell Technologies) and cultured for 4 days. The cells were briefly centrifuged at 300 x g for 4 minutes and the supernatants were collected. The amount of bridging protein was measured in an ELISA assay as described above.

Cytotoxicity assays

Target tumor cell lines were stably transfected with a luciferase cDNA. Cells were seeded at $1x10^4$/25 µl cells per well in a 96 well round (suspension) or opaque flat (adherent) bottom plate in RPMI 1640 containing 10% FBS, without antibiotics. When included, dilutions of bridging proteins were made in 100 µl media and added to the cells. CAR T cells were thawed, washed once with media and recovered via centrifugation at 550 x g for 10 minutes at 4ºC. CAR T cells were added to the wells containing target cells to give an effector:target cell ratio as indicated, in a volume of 25 µl. In experiments using the standard CAR-CD19 T cells, bridging proteins were added as noted. The plates were incubated at 37ºC for 48 hours. For suspension cells, the plate was centrifuged at 550 x g for 5 minutes at room temperature, the pellet was rinsed with PBS, spun again, then lysed with 20 µl 1x lysis buffer (Promega). The lysate was transferred into a 96 well opaque tissue culture plate (Thermo Fisher). For adherent cell lines, the cell culture supernatant was removed, the cells were washed twice with cold PBS and then the 1x lysis buffer was added to the well. For the cytotoxicity assay the plates were read, post injection of luciferin from the detection kit, using a luminometer with an injector (Glomax Multi Detection System, Promega, Madison, WI). The percent killing was calculated based upon the average loss of luminescence of the experimental condition relative to the control wells containing only target cells.

Order of addition assay

Target tumor cell lines Nalm6 and SKOV3 cells were seeded at 1 x 10^4 cells per well in 50 µl in a 96 well round bottom plate for Nalm6 and 96 well white opaque plate for SKOV in

RPMI 1640 containing 10% FBS without antibiotics. Proteins were applied at final concentration of 1 μg/ml in 25 μl media per well. CAR-CD19 T cells were thawed, washed once with media and recovered via centrifugation at 550 x g for 10 minutes at 4ºC. The CAR T cells were applied to the well at a 10:1 ratio to the target cells in 25 μl volume. Three conditions were applied as following: (1) the target cell, the bridging protein and the CAR T cells were added simultaneously, (2) the target protein and the bridging protein were preincubated at 37ºC for 10 minutes then the CAR T cells were added, (3) the bridging protein and CAR T cells were preincubated at 37ºC for 10 minutes then added to the target cells. The plates were incubated at 37ºC for 48 hours. The extent of cytotoxicity was determined as described above.

Restimulation assay

On day 0, the CAR T and target cell cultures were set up at 2:1 (CD3+ CAR T: target cells at $2x10^4$: $1x10^4$ cells/well), and incubated for 48 hours with mitomycin C (MMC) treated Raji or SKOV3 cells, or without activating cells. The target cells were treated with 5 mg/ml MMC (#BP2531-2, Fisher Scientific) for 90 minutes at 37ºC and then washed twice with RPMI medium before adding to the T cells at a 2:1 ratio (CAR T:MMC treated cells). Before each restimulation, 100 μl of media was removed and 100 μl of MMC treated Raji or SKOV3 cells in fresh media were added on days 4, 8 and 12. Using this rest/restimulation sequence the CAR T cells were re-stimulated every 4 days with mitomycin C (MMC) treated Raji or SKOV3 cells. Prior to each restimulation, parallel killing assays were set up on day 4 (after 1 round of restimulation) and day 12 (after 3 rounds of restimulation). For cytotoxicity assays the CAR T cells were counted, pooled, spun at 500 x g for 10 minutes and then resuspended at $5x10^5$

cells/ml. The cytotoxicity assay was set up as described above on JeKo-1 and SKOV3 cells at a 5:1 E:T ratio based on the total T cell count.

In vivo modeling

Animal efficacy models were performed under an institutional IACUC protocol (Cummings School of Veterinary Medicine at Tufts University, Grafton, MA). Each individual study was approved by the Cummings School of Veterinary Medicine IACUC committee and assigned a specific protocol number to aid in tracking compliance in accordance with AAALC guidelines. For all studies the following criteria were used to monitor animal health and allow for humane euthanasia as needed. Lethargy, poor coat condition, poor body condition, abnormal ambulation, and weight loss (>10%) were general health parameters used to determine a euthanasia endpoint. In addition, in the subcutaneous solid tumor studies, mice were euthanized if the tumor mass reached 1500mm3. Any animals reaching any endpoint criterion were euthanized on the same day. No animals died prior to meeting the criteria for euthanasia

The half-life of the wildtype CD19-anti-Her2 bridging protein was determined using SCID mice (n=10) injected IV or IP with 10 mg/kg of protein. Blood samples were taken just prior to injection and at 30 minutes, 90 minutes, 6 hours, 24 hours, 48 hours, 72 hours, 96 hours and 120 hours. Whole blood was collected via the tail vein (100 μL per bleed). Whole blood was collected into EDTA K3 tubes (#411504105, Sarstedt, Numbrecht, Germany). The blood samples were spun for 10 minutes at 8500 rpm. The plasma was then transferred to a 1.5mL eppendorf tubes and frozen until analysis by ELISA as described above. ELISA calculations assumed a 2 ml mouse total blood volume of distribution. The half-life was calculated using the formula $N(t)=N0(1/2)t/t\ ½$ where N(t) is the quantity that remains, N0 is the initial amount, and t = time.

NOD/Scid x common-gamma chain-deficient (NSG) mice were purchased (Jackson Laboratories, Bar Harbor, ME) and allowed to acclimate in cage details for at least 3 days after receipt.

To establish a systemic leukemia model, NSG mice were injected IV with 1 x 10^6 Nalm6-luciferase cells on day one. Luciferase activity was monitored by the injection of luciferin (150mg/kg) followed by immediate whole animal imaging. Leukemia cells were allowed to engraft and expand for 4 days. The baseline degree of luminescence was established by imaging (IVIS 200, Perkin Elmer, Waltham, MA), and mice were randomized into experimental cohorts. There were 10 mice per cohort (n=10) unless otherwise indicated. Mice were injected with CAR T cells on day 4 and imaged weekly to determine the extent of disease burden. Animals were sacrificed when tumor burden or animal health indicated, per the IACUC protocol.

To establish a solid tumor model we implanted 1 x 10^6 SKOV3-luciferase cells subcutaneously in the flank and allowed the tumors to grow to a palpable size of ~150mm^3 on average. Mice were then randomized and CAR T cells were injected IV the following day. There were 10 mice per cohort (n=10) unless otherwise indicated. Caliper measurements of tumor volume were taken 2x weekly. Animals were sacrificed when tumor burden or animal health indicated, per the IACUC protocol. In the rechallenge model, mice that had cleared the SKOV3 tumors were injected ewith Nalm6 cells as described above.

References

1. O'Leary MC, Lu X, Huang Y, Lin X, Mahmood I, Przepiorka D, et al. FDA Approval Summary: Tisagenlecleucel for Treatment of Patients with Relapsed or Refractory B-cell Precursor Acute

Lymphoblastic Leukemia. Clin Cancer Res. 2019;25(4):1142-6. Epub 2018/10/13. doi: 10.1158/1078-0432.CCR-18-2035. PubMed PMID: 30309857.
2. Bouchkouj N, Kasamon YL, de Claro RA, George B, Lin X, Lee S, et al. FDA Approval Summary: Axicabtagene Ciloleucel for Relapsed or Refractory Large B-cell Lymphoma. Clin Cancer Res. 2019;25(6):1702-8. Epub 2018/11/11. doi: 10.1158/1078-0432.CCR-18-2743. PubMed PMID: 30413526.
3. Dai X, Mei Y, Cai D, Han W. Standardizing CAR-T therapy: Getting it scaled up. Biotechnol Adv. 2019;37(1):239-45. Epub 2018/12/14. doi: 10.1016/j.biotechadv.2018.12.002. PubMed PMID: 30543841.
4. Alabanza L, Pegues M, Geldres C, Shi V, Wiltzius JJW, Sievers SA, et al. Function of Novel Anti-CD19 Chimeric Antigen Receptors with Human Variable Regions Is Affected by Hinge and Transmembrane Domains. Mol Ther. 2017;25(11):2452-65. Epub 2017/08/16. doi: 10.1016/j.ymthe.2017.07.013. PubMed PMID: 28807568; PubMed Central PMCID: PMCPMC5675490.
5. Qin H, Ramakrishna S, Nguyen S, Fountaine TJ, Ponduri A, Stetler-Stevenson M, et al. Preclinical Development of Bivalent Chimeric Antigen Receptors Targeting Both CD19 and CD22. Mol Ther Oncolytics. 2018;11:127-37. Epub 2018/12/26. doi: 10.1016/j.omto.2018.10.006. PubMed PMID: 30581986; PubMed Central PMCID: PMCPMC6300726.
6. Schneider D, Xiong Y, Wu D, Nlle V, Schmitz S, Haso W, et al. A tandem CD19/CD20 CAR lentiviral vector drives on-target and off-target antigen modulation in leukemia cell lines. J Immunother Cancer. 2017;5:42. Epub 2017/05/19. doi: 10.1186/s40425-017-0246-1. PubMed PMID: 28515942; PubMed Central PMCID: PMCPMC5433150.
7. Chmielewski M, Abken H. TRUCKs: the fourth generation of CARs. Expert Opin Biol Ther. 2015;15(8):1145-54. Epub 2015/05/20. doi: 10.1517/14712598.2015.1046430. PubMed PMID: 25985798.
8. Choi BD, Yu X, Castano AP, Bouffard AA, Schmidts A, Larson RC, et al. CAR-T cells secreting BiTEs circumvent antigen escape without detectable toxicity. Nat Biotechnol. 2019;37(9):1049-58. Epub 2019/07/25. doi: 10.1038/s41587-019-0192-1. PubMed PMID: 31332324.
9. Neelapu SS. Managing the toxicities of CAR T-cell therapy. Hematol Oncol. 2019;37 Suppl 1:48-52. Epub 2019/06/13. doi: 10.1002/hon.2595. PubMed PMID: 31187535.
10. Ying Z, Huang XF, Xiang X, Liu Y, Kang X, Song Y, et al. A safe and potent anti-CD19 CAR T cell therapy. Nat Med. 2019;25(6):947-53. Epub 2019/04/24. doi: 10.1038/s41591-019-0421-7. PubMed PMID: 31011207.
11. Duong MT, Collinson-Pautz MR, Morschl E, Lu A, Szymanski SP, Zhang M, et al. Two-Dimensional Regulation of CAR-T Cell Therapy with Orthogonal Switches. Mol Ther Oncolytics. 2019;12:124-37. Epub 2019/02/12. doi: 10.1016/j.omto.2018.12.009. PubMed PMID: 30740516; PubMed Central PMCID: PMCPMC6357218.
12. Mestermann K, Giavridis T, Weber J, Rydzek J, Frenz S, Nerreter T, et al. The tyrosine kinase inhibitor dasatinib acts as a pharmacologic on/off switch for CAR T cells. Sci Transl Med. 2019;11(499). Epub 2019/07/05. doi: 10.1126/scitranslmed.aau5907. PubMed PMID: 31270272.
13. Park JH, Geyer MB, Brentjens RJ. CD19-targeted CAR T-cell therapeutics for hematologic malignancies: interpreting clinical outcomes to date. Blood. 2016;127(26):3312-20. Epub 2016/05/22. doi: 10.1182/blood-2016-02-629063. PubMed PMID: 27207800; PubMed Central PMCID: PMCPMC4929923.
14. Finney OC, Brakke HM, Rawlings-Rhea S, Hicks R, Doolittle D, Lopez M, et al. CD19 CAR T cell product and disease attributes predict leukemia remission durability. J Clin Invest. 2019;129(5):2123-32. Epub 2019/03/13. doi: 10.1172/JCI125423. PubMed PMID: 30860496; PubMed Central PMCID: PMCPMC6486329.
15. Forsberg MH, Das A, Saha K, Capitini CM. The potential of CAR T therapy for relapsed or refractory pediatric and young adult B-cell ALL. Ther Clin Risk Manag. 2018;14:1573-84. Epub

2018/09/21. doi: 10.2147/TCRM.S146309. PubMed PMID: 30233192; PubMed Central PMCID: PMCPMC6130274.
16. Lee DW, Kochenderfer JN, Stetler-Stevenson M, Cui YK, Delbrook C, Feldman SA, et al. T cells expressing CD19 chimeric antigen receptors for acute lymphoblastic leukaemia in children and young adults: a phase 1 dose-escalation trial. Lancet. 2015;385(9967):517-28. Epub 2014/10/17. doi: 10.1016/S0140-6736(14)61403-3. PubMed PMID: 25319501.
17. Knochelmann HM, Smith AS, Dwyer CJ, Wyatt MM, Mehrotra S, Paulos CM. CAR T Cells in Solid Tumors: Blueprints for Building Effective Therapies. Front Immunol. 2018;9:1740. Epub 2018/08/25. doi: 10.3389/fimmu.2018.01740. PubMed PMID: 30140266; PubMed Central PMCID: PMCPMC6094980.
18. Klesmith JR, Su L, Wu L, Schrack IA, Dufort FJ, Birt A, et al. Retargeting CD19 Chimeric Antigen Receptor T Cells via Engineered CD19-Fusion Proteins. Mol Pharm. 2019;16(8):3544-58. Epub 2019/06/27. doi: 10.1021/acs.molpharmaceut.9b00418. PubMed PMID: 31242389.
19. De Oliveira SN, Wang J, Ryan C, Morrison SL, Kohn DB, Hollis RP. A CD19/Fc fusion protein for detection of anti-CD19 chimeric antigen receptors. J Transl Med. 2013;11:23. Epub 2013/01/31. doi: 10.1186/1479-5876-11-23. PubMed PMID: 23360526; PubMed Central PMCID: PMCPMC3623748.
20. Ajina A, Maher J. Strategies to Address Chimeric Antigen Receptor Tonic Signaling. Mol Cancer Ther. 2018;17(9):1795-815. Epub 2018/09/06. doi: 10.1158/1535-7163.MCT-17-1097. PubMed PMID: 30181329; PubMed Central PMCID: PMCPMC6130819.
21. Tedder TF, Zhou LJ, Engel P. The CD19/CD21 signal transduction complex of B lymphocytes. Immunol Today. 1994;15(9):437-42. Epub 1994/09/01. doi: 10.1016/0167-5699(94)90274-7. PubMed PMID: 7524521.
22. Sato S, Miller AS, Howard MC, Tedder TF. Regulation of B lymphocyte development and activation by the CD19/CD21/CD81/Leu 13 complex requires the cytoplasmic domain of CD19. J Immunol. 1997;159(7):3278-87. Epub 1997/10/08. PubMed PMID: 9317126.
23. Wang D, Starr R, Alizadeh D, Yang X, Forman SJ, Brown CE. In Vitro Tumor Cell Rechallenge For Predictive Evaluation of Chimeric Antigen Receptor T Cell Antitumor Function. J Vis Exp. 2019;(144). Epub 2019/03/19. doi: 10.3791/59275. PubMed PMID: 30882787; PubMed Central PMCID: PMCPMC6719706.
24. Garcia-Cozar FJ, Molina IJ, Cuadrado MJ, Marubayashi M, Pena J, Santamaria M. Defective B7 expression on antigen-presenting cells underlying T cell activation abnormalities in systemic lupus erythematosus (SLE) patients. Clin Exp Immunol. 1996;104(1):72-9. Epub 1996/04/01. doi: 10.1046/j.1365-2249.1996.d01-648.x. PubMed PMID: 8603537; PubMed Central PMCID: PMCPMC2200384.
25. Petru E, Sevin BU, Perras J, Boike G, Ramos R, Nguyen H, et al. Comparative chemosensitivity profiles in four human ovarian carcinoma cell lines measuring ATP bioluminescence. Gynecol Oncol. 1990;38(2):155-60. Epub 1990/08/01. doi: 10.1016/0090-8258(90)90032-g. PubMed PMID: 2387529.
26. Porter DL, Hwang WT, Frey NV, Lacey SF, Shaw PA, Loren AW, et al. Chimeric antigen receptor T cells persist and induce sustained remissions in relapsed refractory chronic lymphocytic leukemia. Sci Transl Med. 2015;7(303):303ra139. Epub 2015/09/04. doi: 10.1126/scitranslmed.aac5415. PubMed PMID: 26333935; PubMed Central PMCID: PMCPMC5909068.
27. Fraietta JA, Lacey SF, Orlando EJ, Pruteanu-Malinici I, Gohil M, Lundh S, et al. Determinants of response and resistance to CD19 chimeric antigen receptor (CAR) T cell therapy of chronic lymphocytic leukemia. Nat Med. 2018;24(5):563-71. Epub 2018/05/02. doi: 10.1038/s41591-018-0010-1. PubMed PMID: 29713085; PubMed Central PMCID: PMCPMC6117613.
28. Schultz L, Mackall C. Driving CAR T cell translation forward. Sci Transl Med. 2019;11(481). Epub 2019/03/01. doi: 10.1126/scitranslmed.aaw2127. PubMed PMID: 30814337.

29. Feng K, Liu Y, Guo Y, Qiu J, Wu Z, Dai H, et al. Phase I study of chimeric antigen receptor modified T cells in treating HER2-positive advanced biliary tract cancers and pancreatic cancers. Protein Cell. 2018;9(10):838-47. Epub 2017/07/16. doi: 10.1007/s13238-017-0440-4. PubMed PMID: 28710747; PubMed Central PMCID: PMCPMC6160389.
30. Johnson LA, Scholler J, Ohkuri T, Kosaka A, Patel PR, McGettigan SE, et al. Rational development and characterization of humanized anti-EGFR variant III chimeric antigen receptor T cells for glioblastoma. Sci Transl Med. 2015;7(275):275ra22. Epub 2015/02/20. doi: 10.1126/scitranslmed.aaa4963. PubMed PMID: 25696001; PubMed Central PMCID: PMCPMC4467166.
31. O'Rourke DM, Nasrallah MP, Desai A, Melenhorst JJ, Mansfield K, Morrissette JJD, et al. A single dose of peripherally infused EGFRvIII-directed CAR T cells mediates antigen loss and induces adaptive resistance in patients with recurrent glioblastoma. Sci Transl Med. 2017;9(399). Epub 2017/07/21. doi: 10.1126/scitranslmed.aaa0984. PubMed PMID: 28724573; PubMed Central PMCID: PMCPMC5762203.
32. Brown CE, Alizadeh D, Starr R, Weng L, Wagner JR, Naranjo A, et al. Regression of Glioblastoma after Chimeric Antigen Receptor T-Cell Therapy. N Engl J Med. 2016;375(26):2561-9. Epub 2016/12/29. doi: 10.1056/NEJMoa1610497. PubMed PMID: 28029927; PubMed Central PMCID: PMCPMC5390684.
33. Junghans RP, Ma Q, Rathore R, Gomes EM, Bais AJ, Lo AS, et al. Phase I Trial of Anti-PSMA Designer CAR-T Cells in Prostate Cancer: Possible Role for Interacting Interleukin 2-T Cell Pharmacodynamics as a Determinant of Clinical Response. Prostate. 2016;76(14):1257-70. Epub 2016/06/22. doi: 10.1002/pros.23214. PubMed PMID: 27324746.
34. Savoldo B, Rooney CM, Di Stasi A, Abken H, Hombach A, Foster AE, et al. Epstein Barr virus specific cytotoxic T lymphocytes expressing the anti-CD30zeta artificial chimeric T-cell receptor for immunotherapy of Hodgkin disease. Blood. 2007;110(7):2620-30. Epub 2007/05/18. doi: 10.1182/blood-2006-11-059139. PubMed PMID: 17507664; PubMed Central PMCID: PMCPMC1988944.
35. Ahmed N, Brawley V, Hegde M, Bielamowicz K, Kalra M, Landi D, et al. HER2-Specific Chimeric Antigen Receptor-Modified Virus-Specific T Cells for Progressive Glioblastoma: A Phase 1 Dose-Escalation Trial. JAMA Oncol. 2017;3(8):1094-101. Epub 2017/04/21. doi: 10.1001/jamaoncol.2017.0184. PubMed PMID: 28426845; PubMed Central PMCID: PMCPMC5747970.
36. Castellarin M, Watanabe K, June CH, Kloss CC, Posey AD, Jr. Driving cars to the clinic for solid tumors. Gene Ther. 2018;25(3):165-75. Epub 2018/06/09. doi: 10.1038/s41434-018-0007-x. PubMed PMID: 29880908.
37. Mardiana S, Solomon BJ, Darcy PK, Beavis PA. Supercharging adoptive T cell therapy to overcome solid tumor-induced immunosuppression. Sci Transl Med. 2019;11(495). Epub 2019/06/07. doi: 10.1126/scitranslmed.aaw2293. PubMed PMID: 31167925.
38. Lynn RC, Weber EW, Sotillo E, Gennert D, Xu P, Good Z, et al. c-Jun overexpression in CAR T cells induces exhaustion resistance. Nature. 2019;576(7786):293-300. Epub 2019/12/06. doi: 10.1038/s41586-019-1805-z. PubMed PMID: 31802004; PubMed Central PMCID: PMCPMC6944329.
39. Stampouloglou E, Cheng N, Federico A, Slaby E, Monti S, Szeto GL, et al. Yap suppresses T-cell function and infiltration in the tumor microenvironment. PLoS Biol. 2020;18(1):e3000591. Epub 2020/01/14. doi: 10.1371/journal.pbio.3000591. PubMed PMID: 31929526; PubMed Central PMCID: PMCPMC6980695.
40. Ma L, Dichwalkar T, Chang JYH, Cossette B, Garafola D, Zhang AQ, et al. Enhanced CAR-T cell activity against solid tumors by vaccine boosting through the chimeric receptor. Science. 2019;365(6449):162-8. Epub 2019/07/13. doi: 10.1126/science.aav8692. PubMed PMID: 31296767; PubMed Central PMCID: PMCPMC6800571.
41. Reinhard K, Rengstl B, Oehm P, Michel K, Billmeier A, Hayduk N, et al. An RNA vaccine drives expansion and efficacy of claudin-CAR-T cells against solid tumors. Science. 2020. Epub 2020/01/04. doi: 10.1126/science.aay5967. PubMed PMID: 31896660.

42. Mayya V, Judokusumo E, Abu-Shah E, Neiswanger W, Sachar C, Depoil D, et al. Cutting Edge: Synapse Propensity of Human Memory CD8 T Cells Confers Competitive Advantage over Naive Counterparts. J Immunol. 2019;203(3):601-6. Epub 2019/06/16. doi: 10.4049/jimmunol.1801687. PubMed PMID: 31201237; PubMed Central PMCID: PMCPMC6643047.
43. Cabrita R, Lauss M, Sanna A, Donia M, Skaarup Larsen M, Mitra S, et al. Tertiary lymphoid structures improve immunotherapy and survival in melanoma. Nature. 2020. Epub 2020/01/17. doi: 10.1038/s41586-019-1914-8. PubMed PMID: 31942071.
44. Petitprez F, de Reynies A, Keung EZ, Chen TW, Sun CM, Calderaro J, et al. B cells are associated with survival and immunotherapy response in sarcoma. Nature. 2020. Epub 2020/01/17. doi: 10.1038/s41586-019-1906-8. PubMed PMID: 31942077.
45. Helmink BA, Reddy SM, Gao J, Zhang S, Basar R, Thakur R, et al. B cells and tertiary lymphoid structures promote immunotherapy response. Nature. 2020. Epub 2020/01/17. doi: 10.1038/s41586-019-1922-8. PubMed PMID: 31942075.
46. Knoblich K, Cruz Migoni S, Siew SM, Jinks E, Kaul B, Jeffery HC, et al. The human lymph node microenvironment unilaterally regulates T-cell activation and differentiation. PLoS Biol. 2018;16(9):e2005046. Epub 2018/09/05. doi: 10.1371/journal.pbio.2005046. PubMed PMID: 30180168; PubMed Central PMCID: PMCPMC6122729 following competing interests: S. P. Lee is listed as an inventor on the following patent application/patent families regarding development of CLEC14A CAR T cells: PCT/GB2010/001689 (published as WO2011/027132), PCT/GB2016/050134 (published as WO2016/116760), PCT/GB2017/050686, and PCT/GB2017/050689.
47. Dustin ML. Role of adhesion molecules in activation signaling in T lymphocytes. J Clin Immunol. 2001;21(4):258-63. Epub 2001/08/17. doi: 10.1023/a:1010927208180. PubMed PMID: 11506195.
48. Commins SP, Borish L, Steinke JW. Immunologic messenger molecules: cytokines, interferons, and chemokines. J Allergy Clin Immunol. 2010;125(2 Suppl 2):S53-72. Epub 2009/11/26. doi: 10.1016/j.jaci.2009.07.008. PubMed PMID: 19932918.
49. Fooksman DR, Vardhana S, Vasiliver-Shamis G, Liese J, Blair DA, Waite J, et al. Functional anatomy of T cell activation and synapse formation. Annu Rev Immunol. 2010;28:79-105. Epub 2009/12/09. doi: 10.1146/annurev-immunol-030409-101308. PubMed PMID: 19968559; PubMed Central PMCID: PMCPMC2885351.
50. Greenwald RJ, Freeman GJ, Sharpe AH. The B7 family revisited. Annu Rev Immunol. 2005;23:515-48. Epub 2005/03/18. doi: 10.1146/annurev.immunol.23.021704.115611. PubMed PMID: 15771580.
51. Yang Y, Kohler, M.E., Fry, T.J. Effect of chronic endogenous antigen restimulation on CAR T cell persistence and memory formation. Blood. 2017;130:166.
52. Cheadle EJ, Hawkins RE, Batha H, O'Neill AL, Dovedi SJ, Gilham DE. Natural expression of the CD19 antigen impacts the long-term engraftment but not antitumor activity of CD19-specific engineered T cells. J Immunol. 2010;184(4):1885-96. Epub 2010/01/22. doi: 10.4049/jimmunol.0901440. PubMed PMID: 20089697.
53. DiNofia AM, Maude SL. Chimeric Antigen Receptor T-Cell Therapy Clinical Results in Pediatric and Young Adult B-ALL. Hemasphere. 2019;3(4):e279. Epub 2019/11/15. doi: 10.1097/HS9.0000000000000279. PubMed PMID: 31723849; PubMed Central PMCID: PMCPMC6745916 no relevant conflicts of interest to disclose. SM reports honoraria for advisory boards from Novartis Pharmaceuticals and Kite Pharma, Inc. and institutional funding (research support) from Novartis Pharmaceuticals.
54. Singh N, Frey NV, Grupp SA, Maude SL. CAR T Cell Therapy in Acute Lymphoblastic Leukemia and Potential for Chronic Lymphocytic Leukemia. Curr Treat Options Oncol. 2016;17(6):28. Epub 2016/04/22. doi: 10.1007/s11864-016-0406-4. PubMed PMID: 27098534.

55. Callahan C, Barry A, Fooks-Parker S, Smith L, Baniewicz D, Hobbie W. Pediatric Survivorship: Considerations Following CAR T-Cell Therapy. Clin J Oncol Nurs. 2019;23(2):35-41. Epub 2019/03/19. doi: 10.1188/19.CJON.S1.35-41. PubMed PMID: 30880817.
56. Buitrago J, Adkins S, Hawkins M, Iyamu K, Oort T. Adult Survivorship: Considerations Following CAR T-Cell Therapy. Clin J Oncol Nurs. 2019;23(2):42-8. Epub 2019/03/19. doi: 10.1188/19.CJON.S1.42-48. PubMed PMID: 30880816.
57. El-Hallak M, Binstadt BA, Leichtner AM, Bennett CM, Neufeld EJ, Fuhlbrigge RC, et al. Clinical effects and safety of rituximab for treatment of refractory pediatric autoimmune diseases. J Pediatr. 2007;150(4):376-82. Epub 2007/03/27. doi: 10.1016/j.jpeds.2006.10.067. PubMed PMID: 17382113.
58. Gupta R, Roach C, Hryniewicki AT, Vilke GM, Shatsky RA, Coyne CJ. Management of Chimeric Antigen Receptor (CAR) T-Cell Toxicities: A Review and Guideline for Emergency Providers. J Emerg Med. 2020. Epub 2020/06/01. doi: 10.1016/j.jemermed.2020.04.021. PubMed PMID: 32473867.
59. Wall DA, Krueger J. Chimeric antigen receptor T cell therapy comes to clinical practice. Curr Oncol. 2020;27(Suppl 2):S115-S23. Epub 2020/05/06. doi: 10.3747/co.27.5283. PubMed PMID: 32368181; PubMed Central PMCID: PMCPMC7193999.
60. Wu BX, Song NJ, Riesenberg BP, Li Z. Development of molecular and pharmacological switches for chimeric antigen receptor T cells. Exp Hematol Oncol. 2019;8:27. Epub 2019/11/12. doi: 10.1186/s40164-019-0151-z. PubMed PMID: 31709128; PubMed Central PMCID: PMCPMC6833279.
61. Weber EW, Lynn RC, Sotillo E, Lattin J, Xu P, Mackall CL. Pharmacologic control of CAR-T cell function using dasatinib. Blood Adv. 2019;3(5):711-7. Epub 2019/03/01. doi: 10.1182/bloodadvances.2018028720. PubMed PMID: 30814055; PubMed Central PMCID: PMCPMC6418502.
62. Majzner RG, Mackall CL. Tumor Antigen Escape from CAR T-cell Therapy. Cancer Discov. 2018;8(10):1219-26. Epub 2018/08/24. doi: 10.1158/2159-8290.CD-18-0442. PubMed PMID: 30135176.
63. Timmers M, Roex G, Wang Y, Campillo-Davo D, Van Tendeloo VFI, Chu Y, et al. Chimeric Antigen Receptor-Modified T Cell Therapy in Multiple Myeloma: Beyond B Cell Maturation Antigen. Front Immunol. 2019;10:1613. Epub 2019/08/06. doi: 10.3389/fimmu.2019.01613. PubMed PMID: 31379824; PubMed Central PMCID: PMCPMC6646459.
64. Akhavan D, Alizadeh D, Wang D, Weist MR, Shepphird JK, Brown CE. CAR T cells for brain tumors: Lessons learned and road ahead. Immunol Rev. 2019;290(1):60-84. Epub 2019/07/30. doi: 10.1111/imr.12773. PubMed PMID: 31355493; PubMed Central PMCID: PMCPMC6771592.
65. Bannas P, Hambach J, Koch-Nolte F. Nanobodies and Nanobody-Based Human Heavy Chain Antibodies As Antitumor Therapeutics. Front Immunol. 2017;8:1603. Epub 2017/12/08. doi: 10.3389/fimmu.2017.01603. PubMed PMID: 29213270; PubMed Central PMCID: PMCPMC5702627.
66. Gonzalez-Sapienza G, Rossotti MA, Tabares-da Rosa S. Single-Domain Antibodies As Versatile Affinity Reagents for Analytical and Diagnostic Applications. Front Immunol. 2017;8:977. Epub 2017/09/06. doi: 10.3389/fimmu.2017.00977. PubMed PMID: 28871254; PubMed Central PMCID: PMCPMC5566570.
67. Arndt C, Fasslrinner F, Loureiro LR, Koristka S, Feldmann A, Bachmann M. Adaptor CAR Platforms-Next Generation of T Cell-Based Cancer Immunotherapy. Cancers (Basel). 2020;12(5). Epub 2020/05/28. doi: 10.3390/cancers12051302. PubMed PMID: 32455621; PubMed Central PMCID: PMCPMC7281723.
68. Roybal KT, Rupp LJ, Morsut L, Walker WJ, McNally KA, Park JS, et al. Precision Tumor Recognition by T Cells With Combinatorial Antigen-Sensing Circuits. Cell. 2016;164(4):770-9. Epub 2016/02/03. doi: 10.1016/j.cell.2016.01.011. PubMed PMID: 26830879; PubMed Central PMCID: PMCPMC4752902.
69. Grada Z, Hegde M, Byrd T, Shaffer DR, Ghazi A, Brawley VS, et al. TanCAR: A Novel Bispecific Chimeric Antigen Receptor for Cancer Immunotherapy. Mol Ther Nucleic Acids. 2013;2:e105. Epub

2013/07/11. doi: 10.1038/mtna.2013.32. PubMed PMID: 23839099; PubMed Central PMCID: PMCPMC3731887.
70. Tu S, Zhou X, Guo Z, Huang R, Yue C, He Y, et al. CD19 and CD70 Dual-Target Chimeric Antigen Receptor T-Cell Therapy for the Treatment of Relapsed and Refractory Primary Central Nervous System Diffuse Large B-Cell Lymphoma. Front Oncol. 2019;9:1350. Epub 2019/12/24. doi: 10.3389/fonc.2019.01350. PubMed PMID: 31867275; PubMed Central PMCID: PMCPMC6904344.
71. Balakrishnan A, Rajan A, Salter AI, Kosasih PL, Wu Q, Voutsinas J, et al. Multispecific Targeting with Synthetic Ankyrin Repeat Motif Chimeric Antigen Receptors. Clin Cancer Res. 2019;25(24):7506-16. Epub 2019/09/25. doi: 10.1158/1078-0432.CCR-19-1479. PubMed PMID: 31548346; PubMed Central PMCID: PMCPMC6940018.
72. Guedan S, Calderon H, Posey AD, Jr., Maus MV. Engineering and Design of Chimeric Antigen Receptors. Mol Ther Methods Clin Dev. 2019;12:145-56. Epub 2019/01/23. doi: 10.1016/j.omtm.2018.12.009. PubMed PMID: 30666307; PubMed Central PMCID: PMCPMC6330382.
73. Ellerman D. Bispecific T-cell engagers: Towards understanding variables influencing the in vitro potency and tumor selectivity and their modulation to enhance their efficacy and safety. Methods. 2019;154:102-17. Epub 2018/11/06. doi: 10.1016/j.ymeth.2018.10.026. PubMed PMID: 30395966.
74. Slaney CY, Wang P, Darcy PK, Kershaw MH. CARs versus BiTEs: A Comparison between T Cell-Redirection Strategies for Cancer Treatment. Cancer Discov. 2018;8(8):924-34. Epub 2018/07/18. doi: 10.1158/2159-8290.CD-18-0297. PubMed PMID: 30012854.
75. Goebeler ME, Bargou RC. T cell-engaging therapies - BiTEs and beyond. Nat Rev Clin Oncol. 2020;17(7):418-34. Epub 2020/04/04. doi: 10.1038/s41571-020-0347-5. PubMed PMID: 32242094.
76. Frigault MJ, Dietrich J, Martinez-Lage M, Leick M, Choi BD, DeFilipp Z, et al. Tisagenlecleucel CAR T-cell therapy in secondary CNS lymphoma. Blood. 2019;134(11):860-6. Epub 2019/07/20. doi: 10.1182/blood.2019001694. PubMed PMID: 31320380; PubMed Central PMCID: PMCPMC7022436.
77. He X, Xiao X, Li Q, Jiang Y, Cao Y, Sun R, et al. Anti-CD19 CAR-T as a feasible and safe treatment against central nervous system leukemia after intrathecal chemotherapy in adults with relapsed or refractory B-ALL. Leukemia. 2019;33(8):2102-4. Epub 2019/03/09. doi: 10.1038/s41375-019-0437-5. PubMed PMID: 30846865; PubMed Central PMCID: PMCPMC6756216.
78. Hegde M, Joseph SK, Pashankar F, DeRenzo C, Sanber K, Navai S, et al. Tumor response and endogenous immune reactivity after administration of HER2 CAR T cells in a child with metastatic rhabdomyosarcoma. Nat Commun. 2020;11(1):3549. Epub 2020/07/17. doi: 10.1038/s41467-020-17175-8. PubMed PMID: 32669548; PubMed Central PMCID: PMCPMC7363864.
79. Carter P, Presta L, Gorman CM, Ridgway JB, Henner D, Wong WL, et al. Humanization of an anti-p185HER2 antibody for human cancer therapy. Proc Natl Acad Sci U S A. 1992;89(10):4285-9. Epub 1992/05/15. doi: 10.1073/pnas.89.10.4285. PubMed PMID: 1350088; PubMed Central PMCID: PMCPMC49066.
80. Nicholson IC, Lenton KA, Little DJ, Decorso T, Lee FT, Scott AM, et al. Construction and characterisation of a functional CD19 specific single chain Fv fragment for immunotherapy of B lineage leukaemia and lymphoma. Mol Immunol. 1997;34(16-17):1157-65. Epub 1998/05/05. doi: 10.1016/s0161-5890(97)00144-2. PubMed PMID: 9566763.

Supporting Information

S1 Fig. ELISA assays of bridging protein binding. A) The capture agent was Her2-Fc and the detection agent was anti-CD19 antibody FMC63. B) ELISA assay of bridging protein binding: the capture agent was anti-CD19 antibody FMC63 and the detection agent was biotinylated Her2. In both assays the bridging proteins (#42, #340) bound significantly better than the control proteins (#28, #117); $p < 0.01$ at the bridging protein EC_{50} value.

S2 Fig. Flow cytometric analyses of bridging protein binding. A) Anti-Flag-tag staining of CAR-CD19 transduced donor primary T cells (donor 69, results are representative of n=4 transduction experiments). B) Binding of purified CD19-anti-Her2 bridging proteins to anti-CD19 CAR transduced primary T cells (donor 69, n=2, * $p < 0.004$ for binding of #42 vs #340). C) Expression of antigen Her2 on the ovarian carcinoma cell line SKOV3 (results are representative of n=6 flow cytometry assays). D) Binding of bridging proteins to SKOV3 cells (triplicate wells, the data are from 1 of 2 experiments performed).

S3 Fig. Binding of bridging proteins to SKOV3 and BT474 cell lines. A) Representative gating of SKOV3 cells. B) Binding with 1 µg/ml of control and bridging proteins to SKOV3 cells. C) dose response binding to SKOV3 cells. D) Representative gating of BT474 cells. E) Binding with 1 µg/ml of control and bridging proteins to SKOV3 cells. F) dose response binding to BT474 cells. Detection of bound protein was with anti-CD19-PE antibody except for the CD22-anti-Her2 samples that were detected with anti-CD22-PE antibody.

S4 Fig. Flow cytometric analysis. Analyses of Her2 and EGFR expression on cell lines. A) K562-EGFR cells. B) BT474 cells. C) SKOV3 cells.

S5 Fig. Representative bridging protein flow cytometry data. A) Flow cytometry data showing various bridging proteins binding at saturation (A,C,E) and in dose response curves (B,D,F) to K562-EGFR cells (A,B), BT474 cells (C,D) and SKOV3 cells (E,F), as detected with anti-CD19 antibody FMC63-PE.

S6 Fig. Bridging protein mediated cytotoxicity of EGFR-positive and Her2-positive cell lines. A) K562-EGFR. B) BT474. C) SKOV3. Anti-CD19 CAR T cells (donor 54, 47% Flag-tag positive) were added at an E:T ratio of 10:1. Bridging proteins were added in a dose titration into the cytotoxicity assay.

S7 Fig. Phenotypic analysis of protein expression, and CD19-anti-Her2 bridging protein binding to cell lines. A) SKOV3. B) K562. C) Raji. D) U937. E) OCI-LY3.

S8 Fig. Half-life measurement data. PK measurements of a CD19-anti-Her2 bridging protein after injection into Rag-/- common gamma-/- mice.

S9 Fig. Anti-CD19 CAR T cells control CD19-positive Nalm6 leukemic cell growth *in vivo*. Mice were implanted with Nalm6 cell IV, then treated 4 days later with anti-CD19 CAR T cells (donor 54, 99.5% CD3-positive, 52% Flag-tag positive for CAR expression, and 56% CD8 positive by flow cytometric analyses). A) Representative images, day 12. B) Luminescence measurement, day 12. C) Luminescence measurement, day 19: note only 2 control (UTD) mice were still alive at day 19. The red bar marks the background luminescent reading. UTD lumin readings were statistically higher than treated mice on both days 12 and 19 $p < 0.001$. This experiment is representative of 3 independent experiments.

Figure 1.

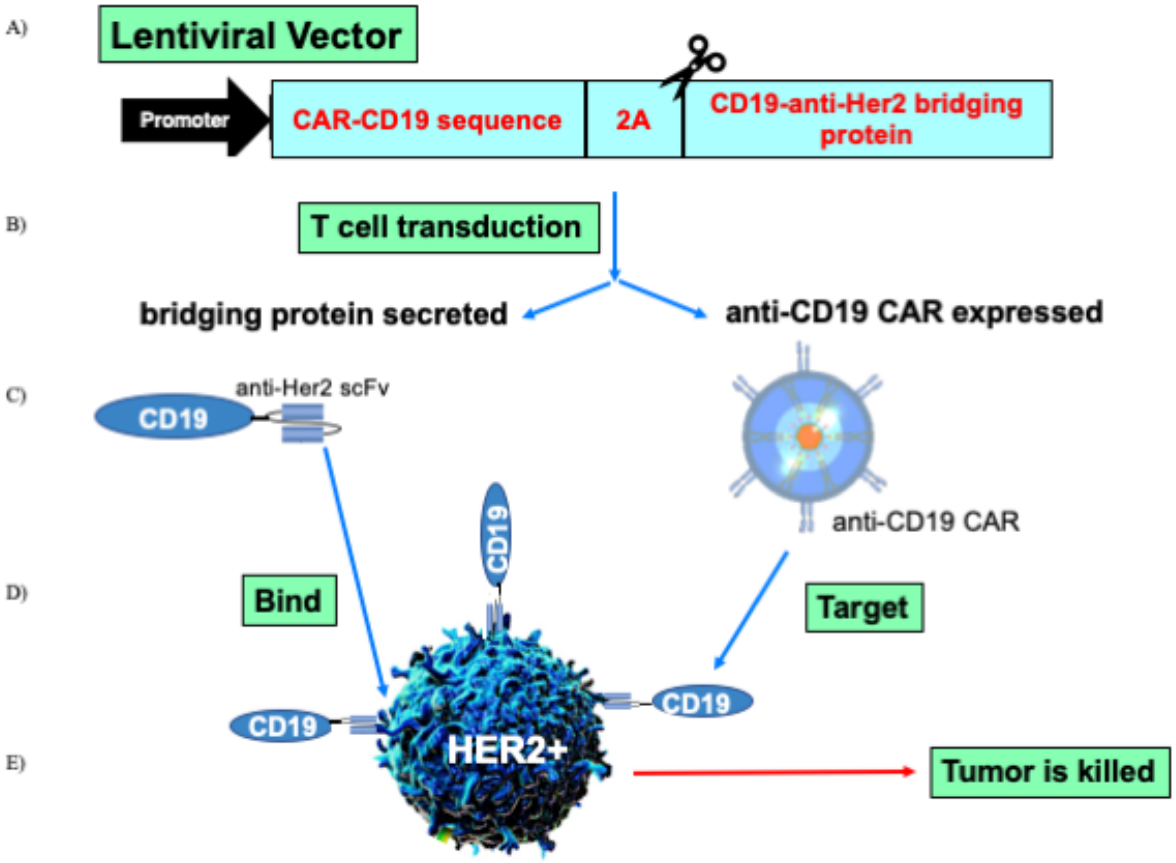
A)
Lentiviral Vector
Promoter
CAR-CD19 sequence
2A
CD19-anti-Her2 bridging protein
B)
T cell transduction
bridging protein secreted
anti-CD19 CAR expressed
C)
anti-Her2 scFv
CD19
anti-CD19 CAR
D)
Bind
Target
CD19
CD19
CD19
E)
HER2+
Tumor is killed

Figure 2.

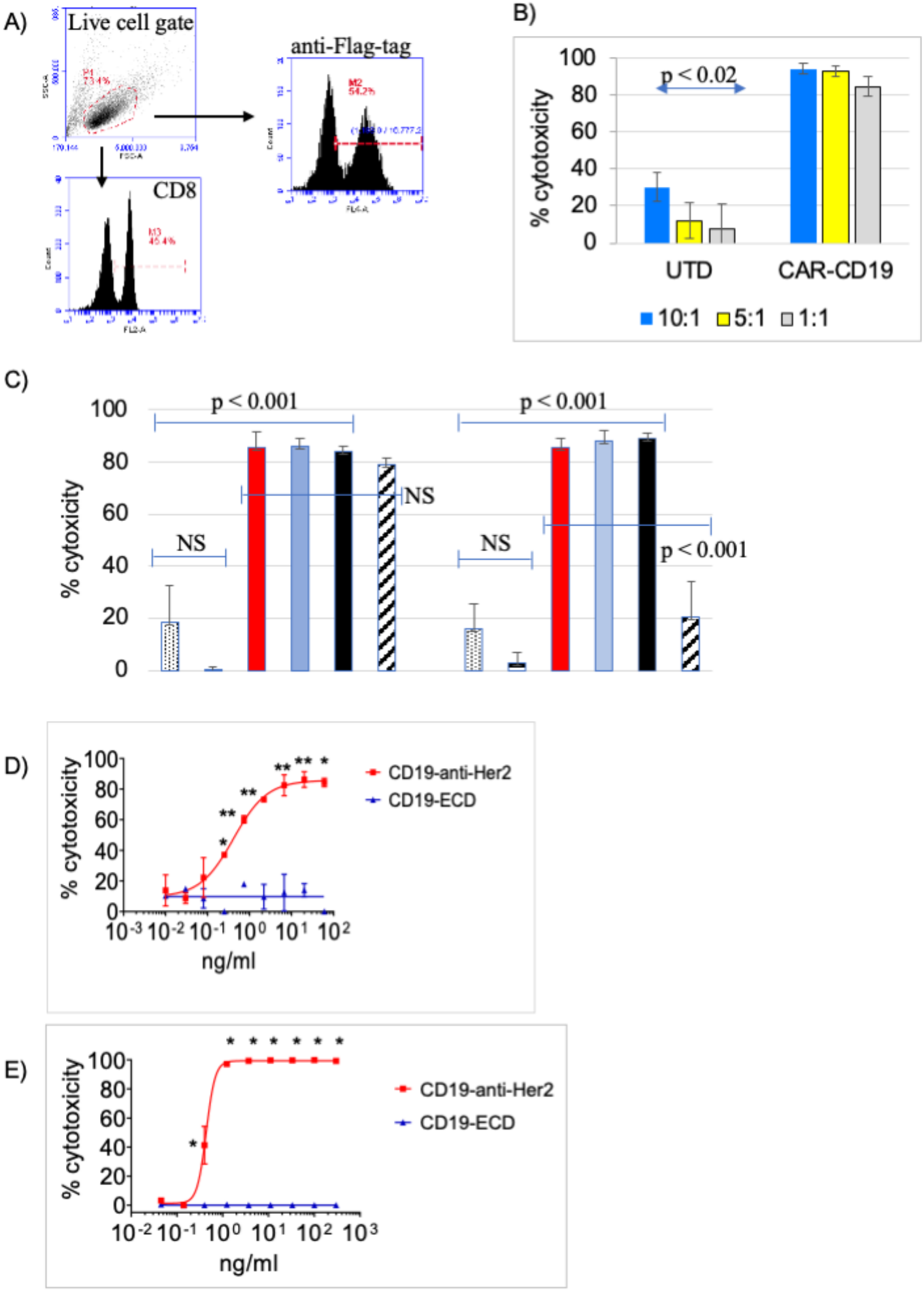
A)
Live cell gate
anti-Flag-tag
CD8
B)
% cytotoxicity
p < 0.02
UTD
CAR-CD19
10:1
5:1
1:1
C)
% cytoxicity
p < 0.001
p < 0.001
NS
NS
NS
p < 0.001
D)
% cytotoxicity
CD19-anti-Her2
CD19-ECD
ng/ml
E)
% cytotoxicity
CD19-anti-Her2
CD19-ECD
ng/ml

Figure 3.

A)

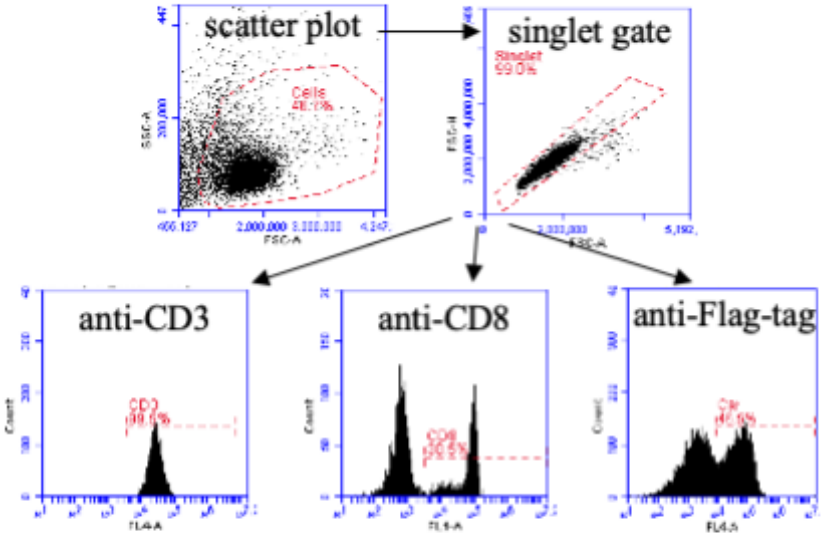
scatter plot
singlet gate
anti-CD3
anti-CD8
anti-Flag-tag

B)

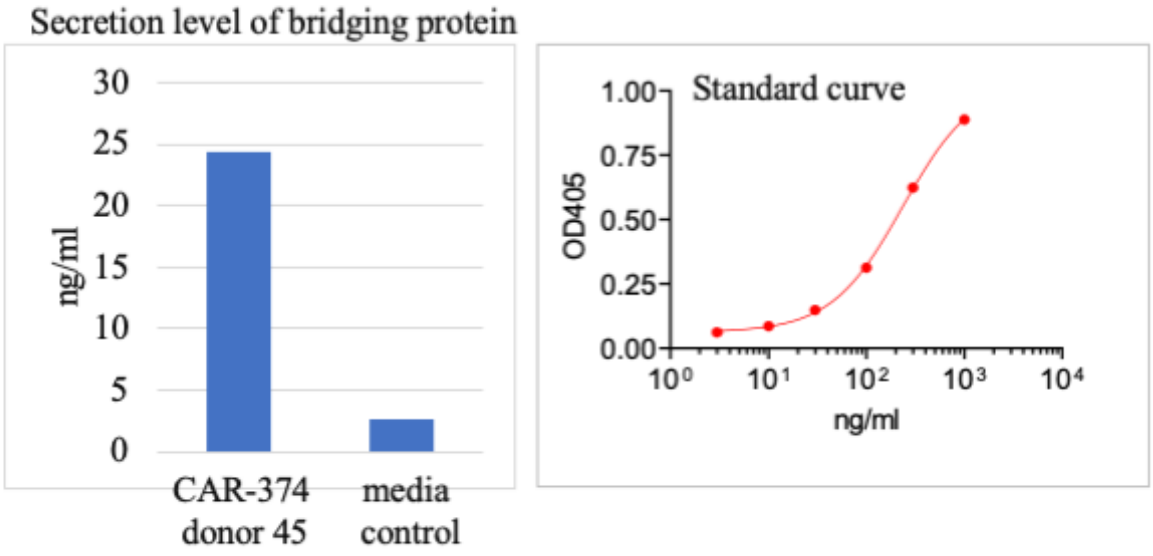
Secretion level of bridging protein
ng/ml
30
25
20
15
10
5
0
CAR-374 donor 45
media control
Standard curve
OD405
1.00
0.75
0.50
0.25
0.00
10^0
10^1
10^2
10^3
10^4
ng/ml

C)

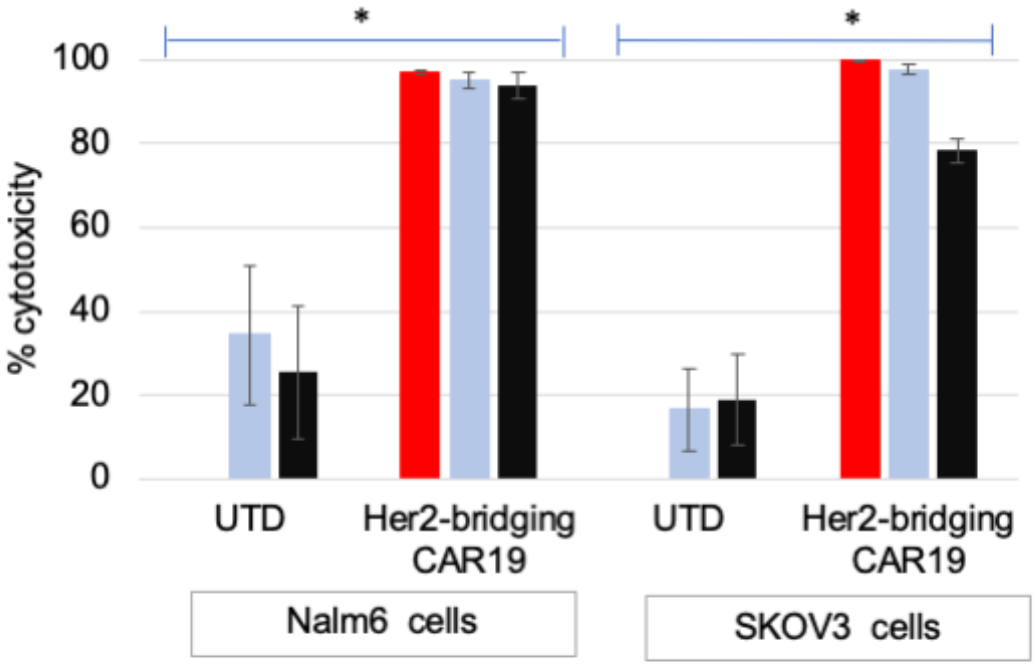
*
*
% cytotoxicity
100
80
60
40
20
0
UTD
Her2-bridging CAR19
UTD
Her2-bridging CAR19
Nalm6 cells
SKOV3 cells

Figure 4

A)

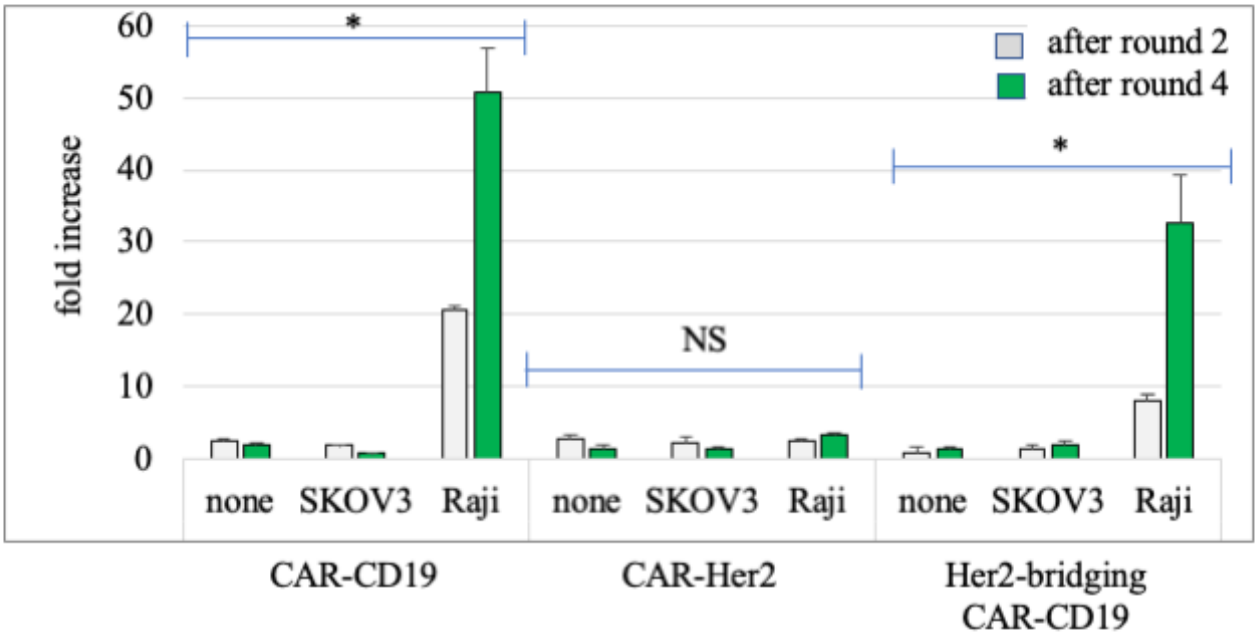
60
50
40
30
20
10
0
fold increase
*
NS
*
after round 2
after round 4
none
SKOV3
Raji
none
SKOV3
Raji
none
SKOV3
Raji
CAR-CD19
CAR-Her2
Her2-bridging CAR-CD19

B)

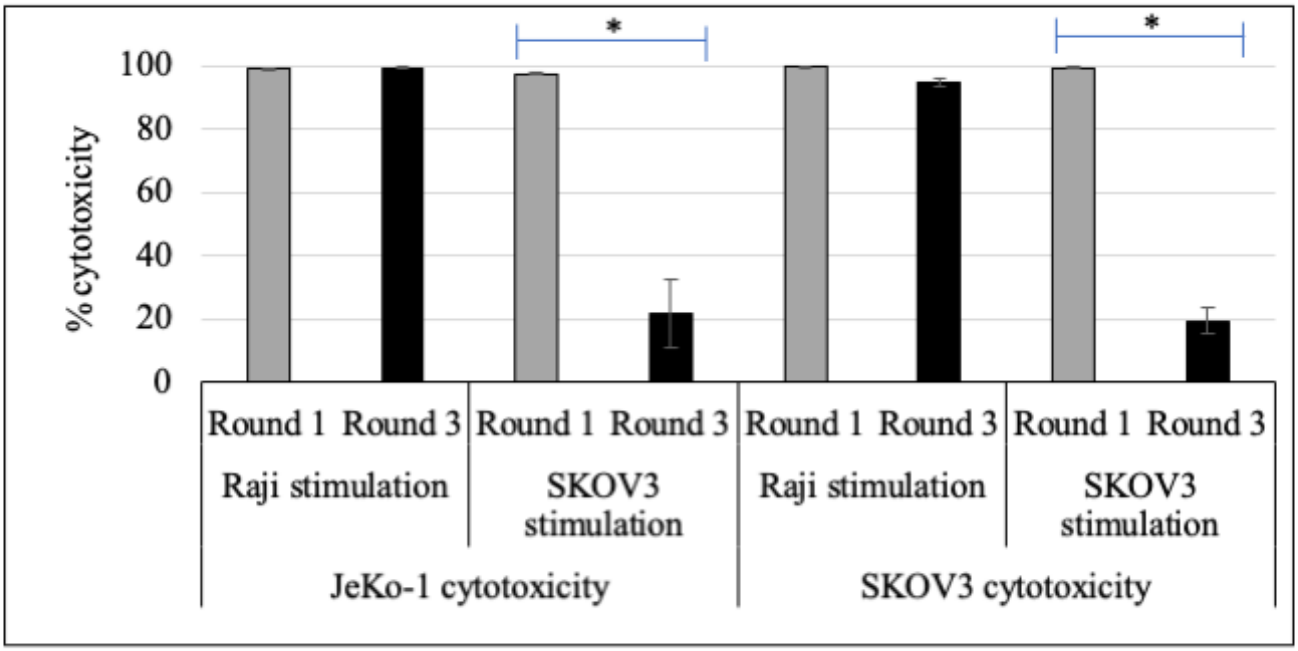
100
80
60
40
20
0
% cytotoxicity
*
*
Round 1
Round 3
Round 1
Round 3
Round 1
Round 3
Round 1
Round 3
Raji stimulation
SKOV3 stimulation
Raji stimulation
SKOV3 stimulation
JeKo-1 cytotoxicity
SKOV3 cytotoxicity

Figure 5.

A)

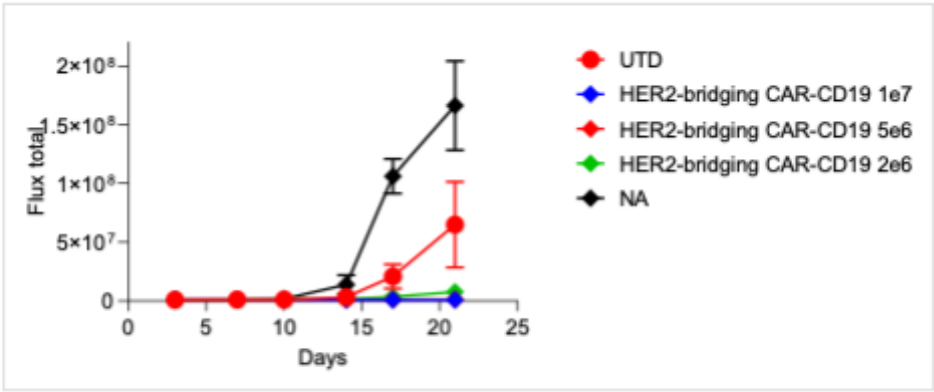

B)

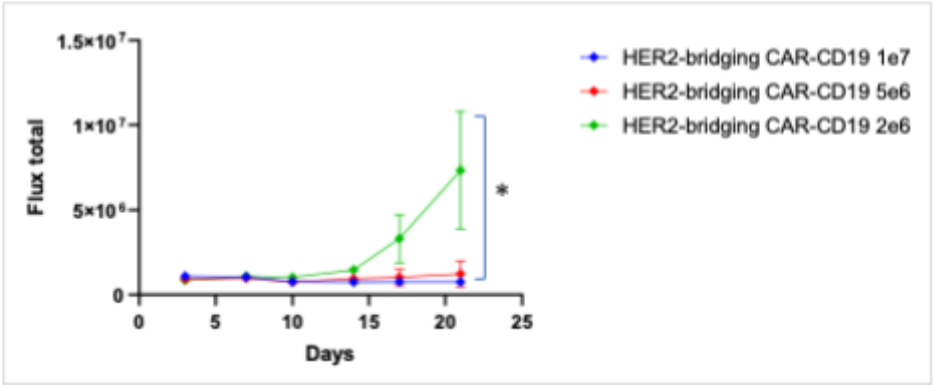

C)

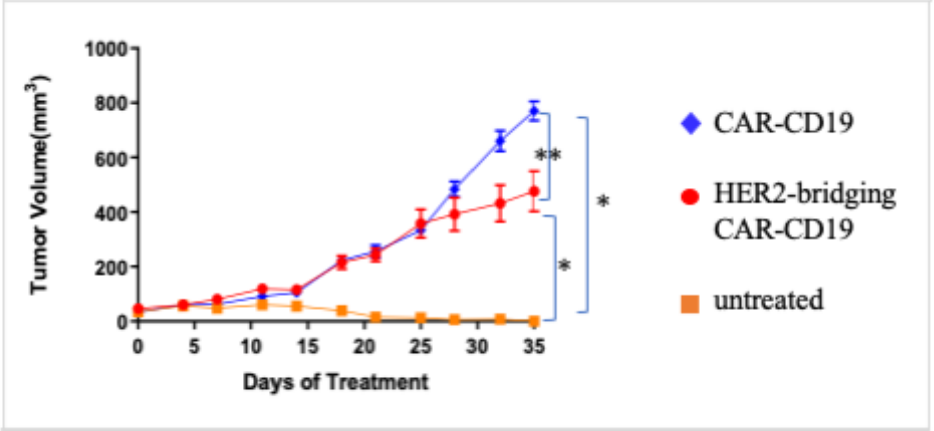

D)

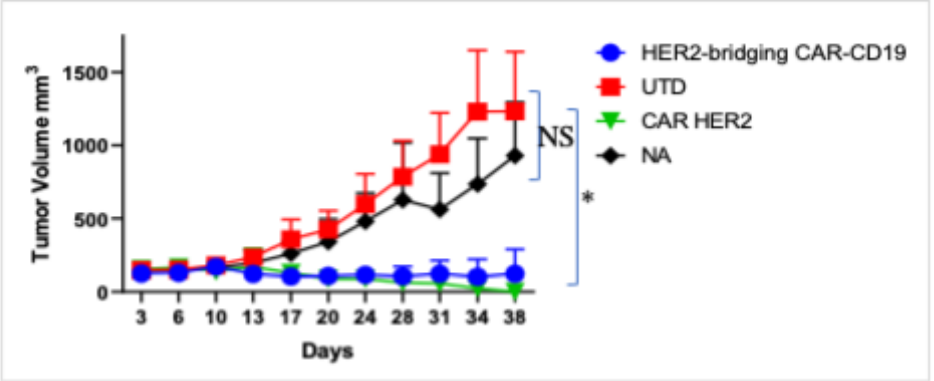

E)

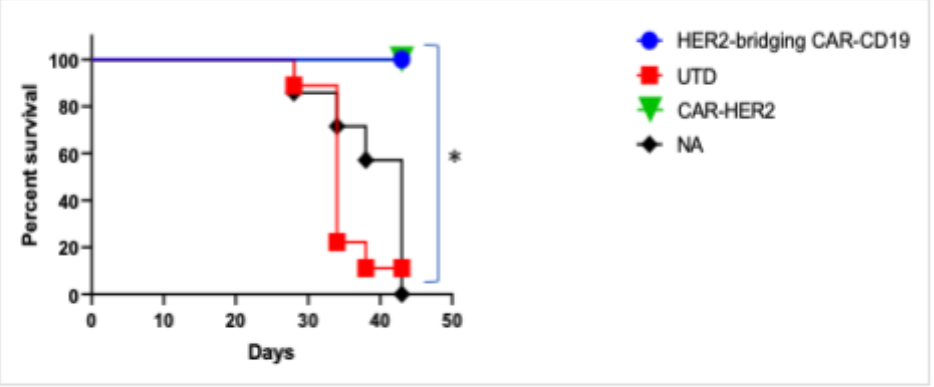

Figure 6.

A)

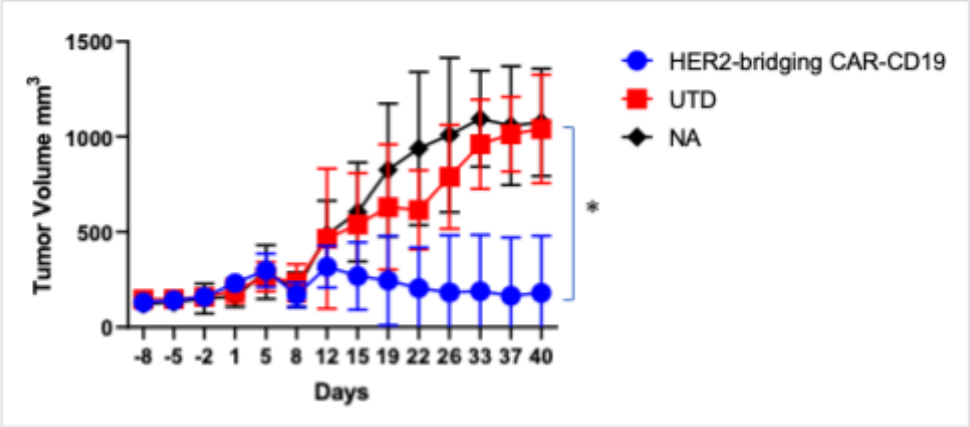
Tumor Volume mm3
1500
1000
500
0
-8 -5 -2 1 5 8 12 15 19 22 26 33 37 40
Days
HER2-bridging CAR-CD19
UTD
NA
*

B)

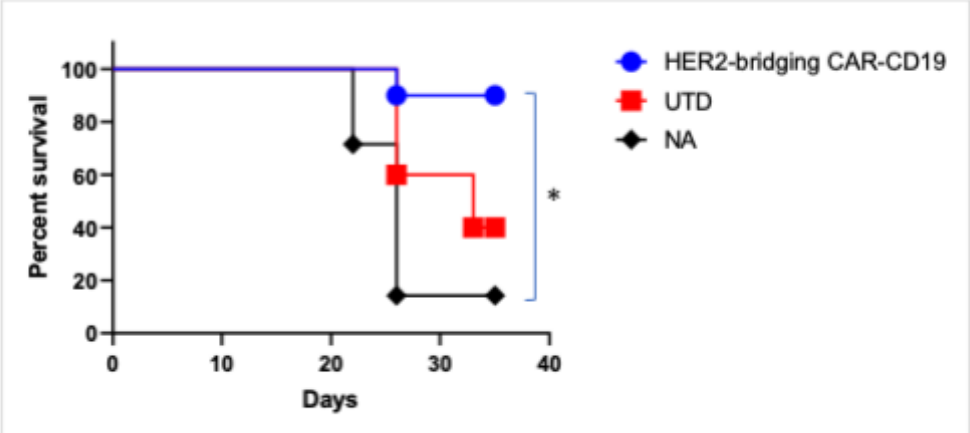
Percent survival
100
80
60
40
20
0
0 10 20 30 40
Days
HER2-bridging CAR-CD19
UTD
NA
*

C)

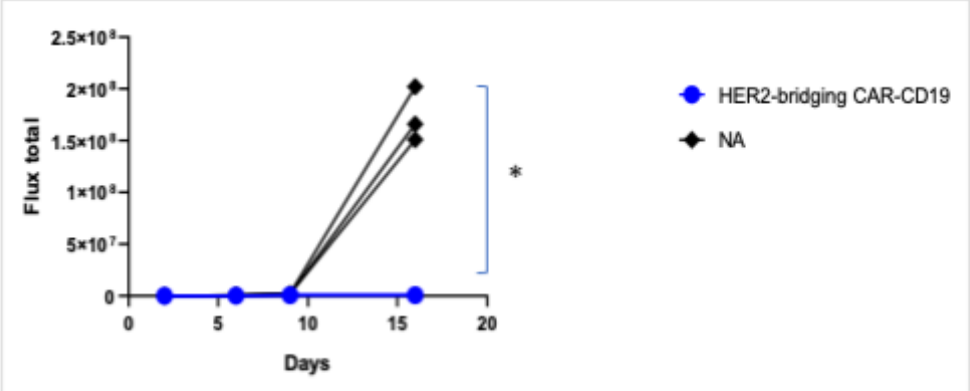
Flux total
2.5×10⁸
2×10⁸
1.5×10⁸
1×10⁸
5×10⁷
0
0 5 10 15 20
Days
HER2-bridging CAR-CD19
NA
*

Figure 1.

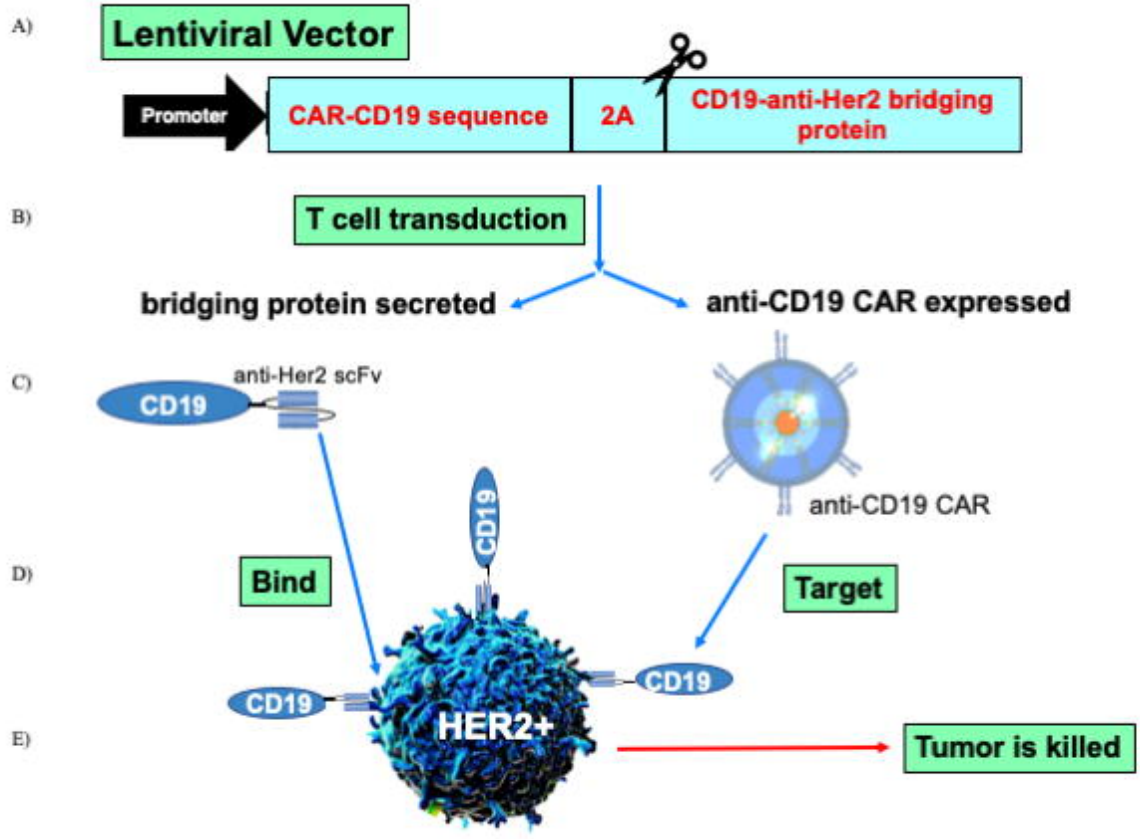
A)
Lentiviral Vector
Promoter
CAR-CD19 sequence
2A
CD19-anti-Her2 bridging protein
B)
T cell transduction
bridging protein secreted
anti-CD19 CAR expressed
C)
anti-Her2 scFv
CD19
anti-CD19 CAR
D)
Bind
Target
CD19
CD19
CD19
E)
HER2+
Tumor is killed

Figure 2.

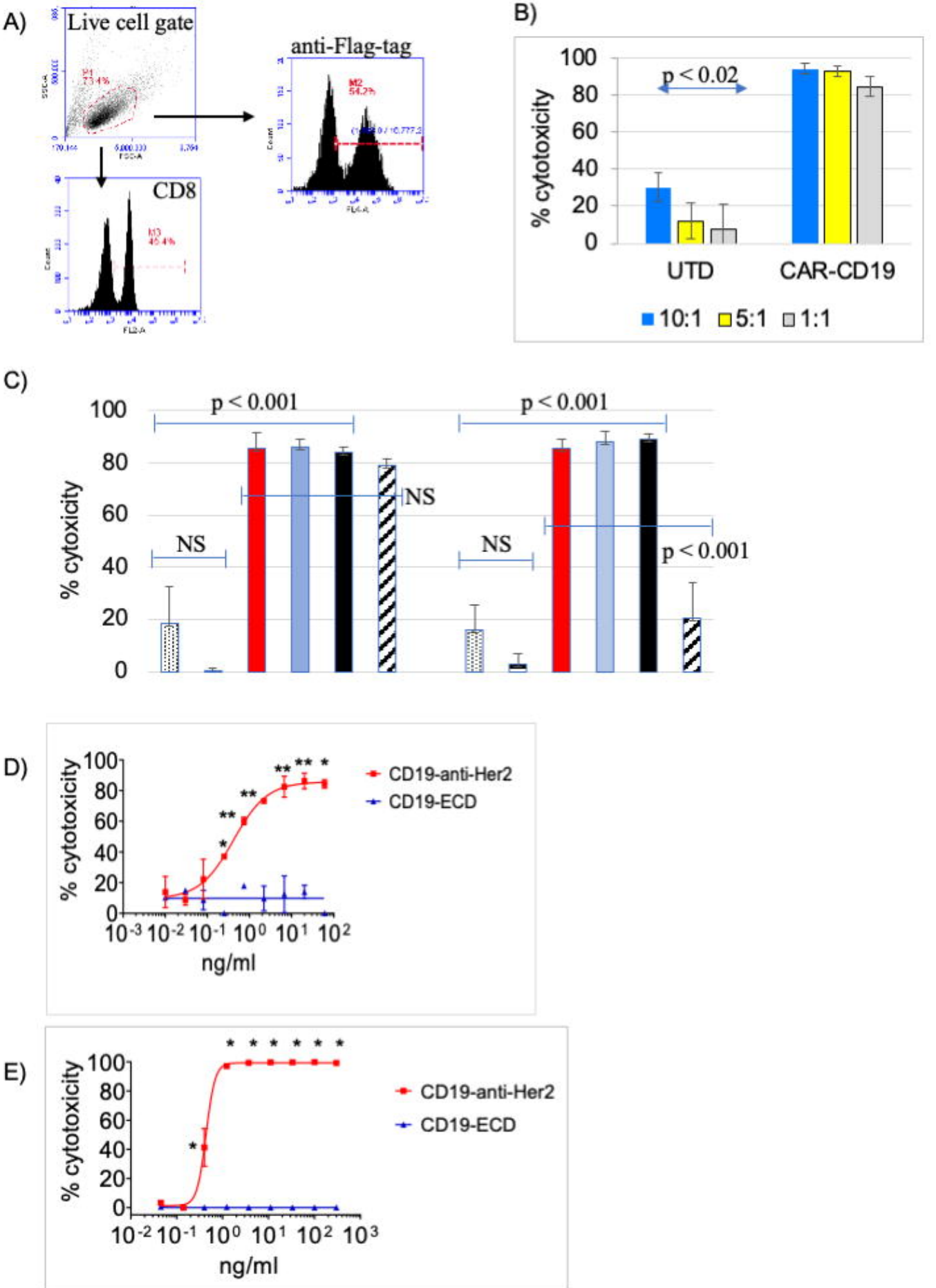
A)
Live cell gate
anti-Flag-tag
CD8
B)
% cytotoxicity
p < 0.02
UTD
CAR-CD19
10:1
5:1
1:1
C)
% cytoxicity
p < 0.001
p < 0.001
NS
NS
NS
p < 0.001
D)
% cytotoxicity
CD19-anti-Her2
CD19-ECD
ng/ml
E)
% cytotoxicity
CD19-anti-Her2
CD19-ECD
ng/ml

Figure 3.

A)

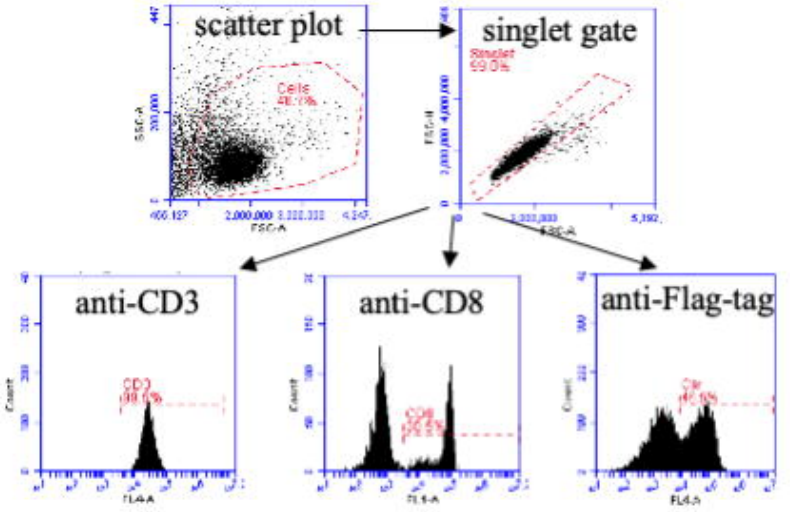
scatter plot
singlet gate
anti-CD3
anti-CD8
anti-Flag-tag

B)

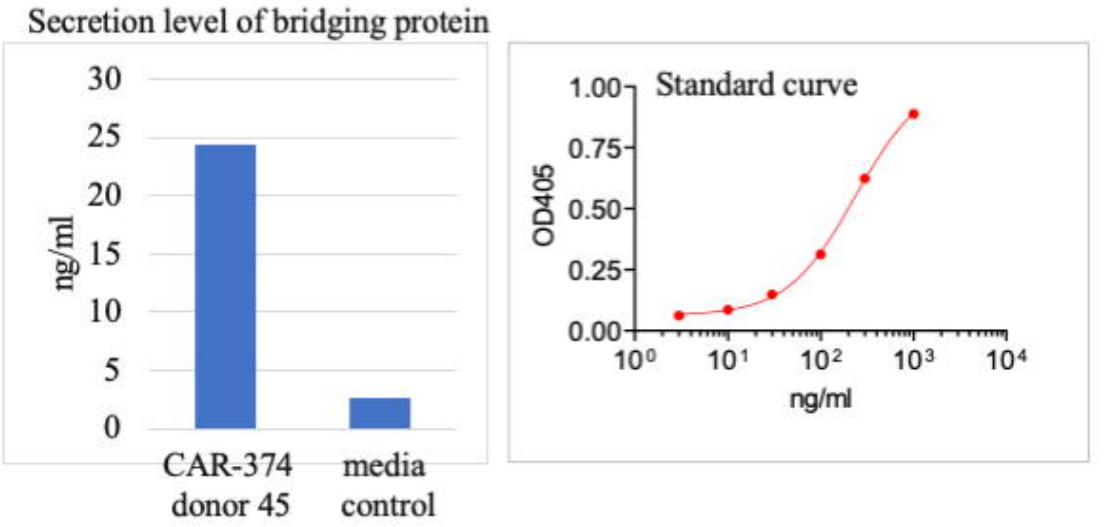
Secretion level of bridging protein
ng/ml
30
25
20
15
10
5
0
CAR-374 donor 45
media control
Standard curve
OD405
1.00
0.75
0.50
0.25
0.00
10^0
10^1
10^2
10^3
10^4
ng/ml

C)

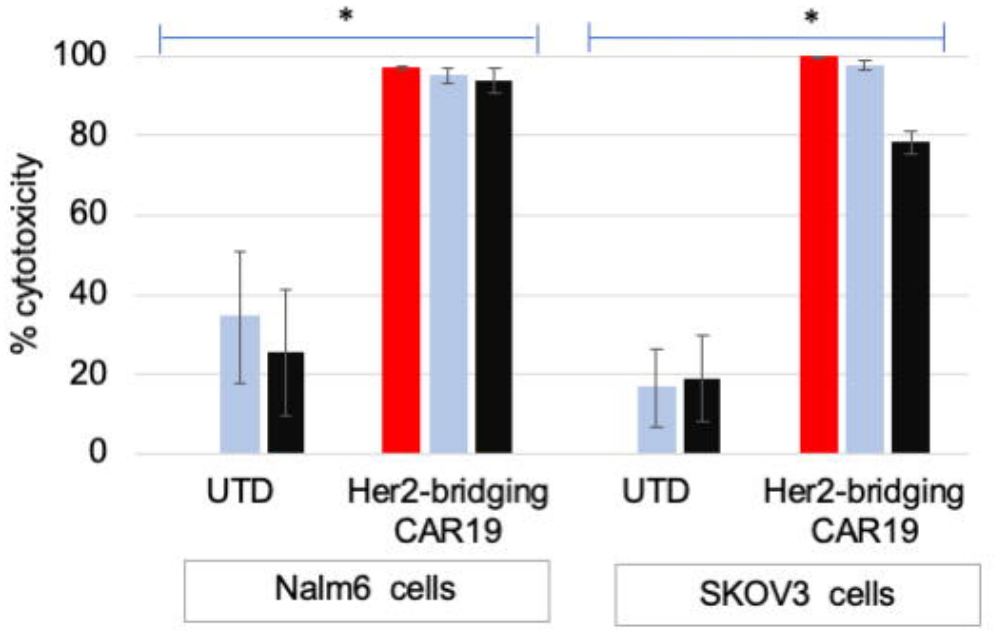
*
*
% cytotoxicity
100
80
60
40
20
0
UTD
Her2-bridging CAR19
UTD
Her2-bridging CAR19
Nalm6 cells
SKOV3 cells

Figure 4

A)

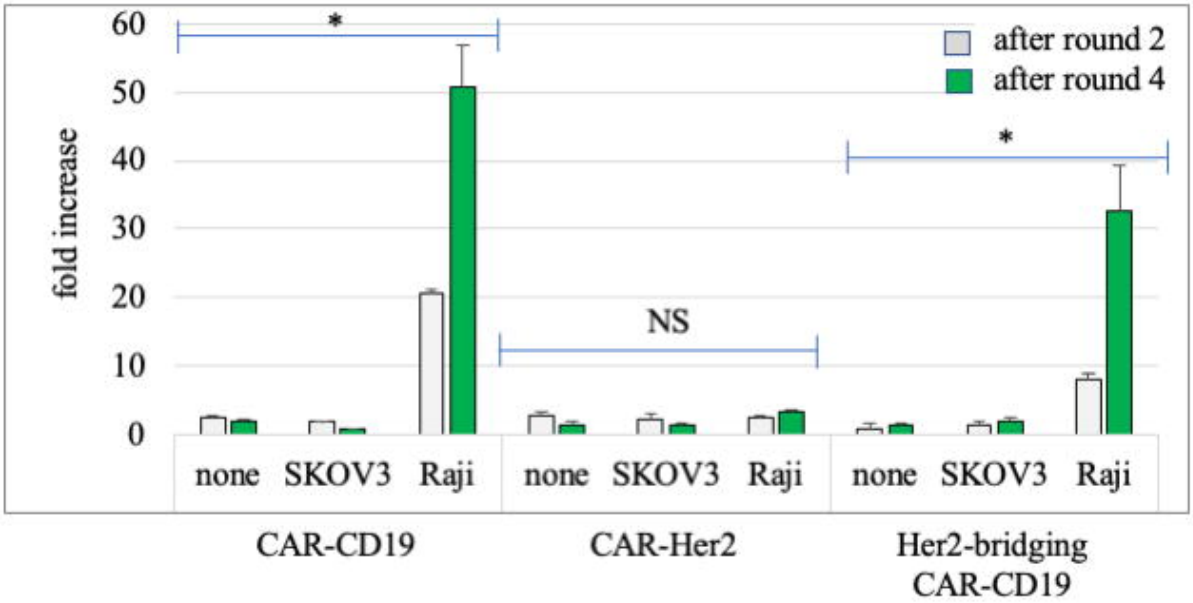
60
50
40
30
20
10
0
fold increase
*
NS
*
after round 2
after round 4
none
SKOV3
Raji
none
SKOV3
Raji
none
SKOV3
Raji
CAR-CD19
CAR-Her2
Her2-bridging CAR-CD19

B)

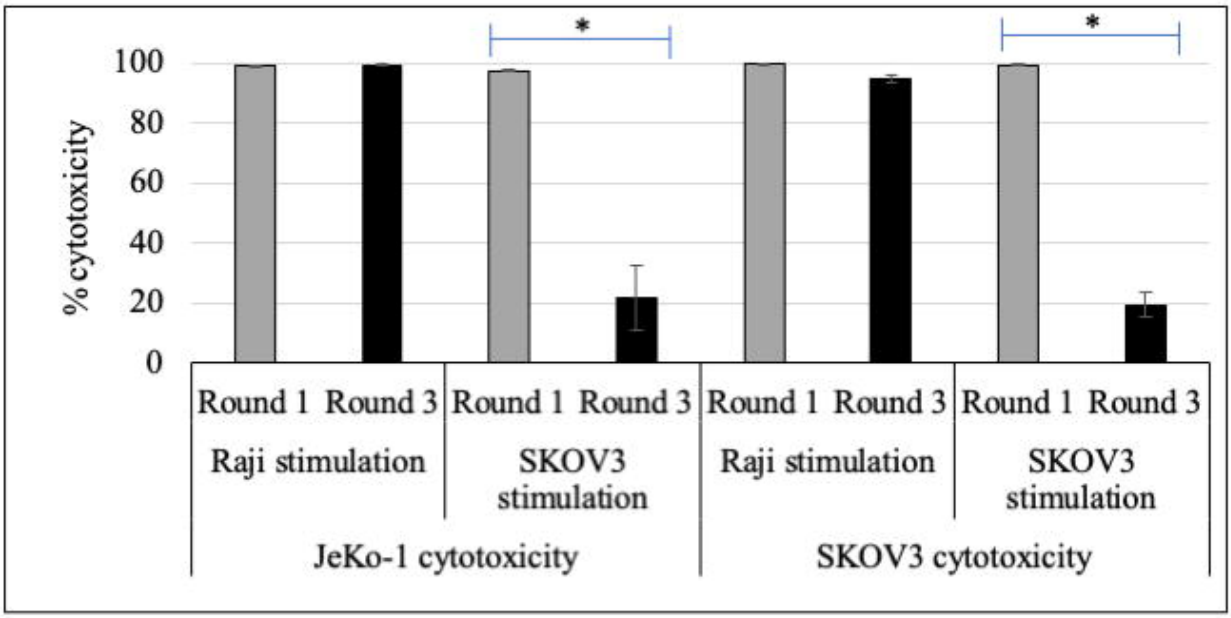
100
80
60
40
20
0
% cytotoxicity
*
*
Round 1
Round 3
Round 1
Round 3
Round 1
Round 3
Round 1
Round 3
Raji stimulation
SKOV3 stimulation
Raji stimulation
SKOV3 stimulation
JeKo-1 cytotoxicity
SKOV3 cytotoxicity

Figure 5.

A)

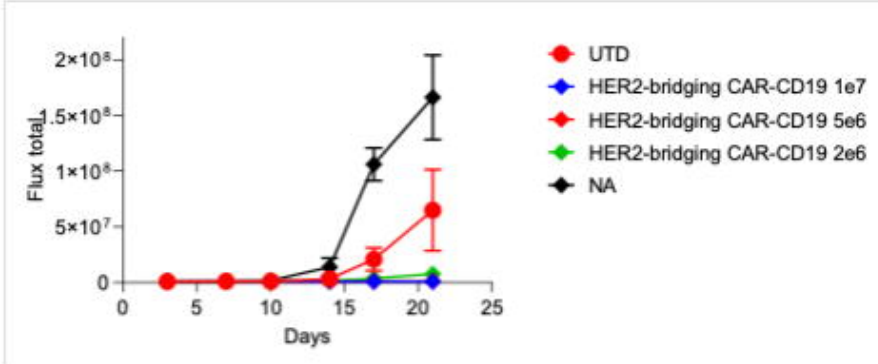

B)

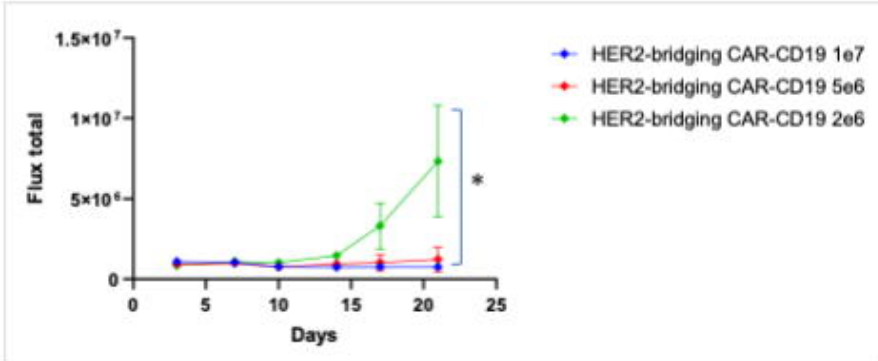

C)

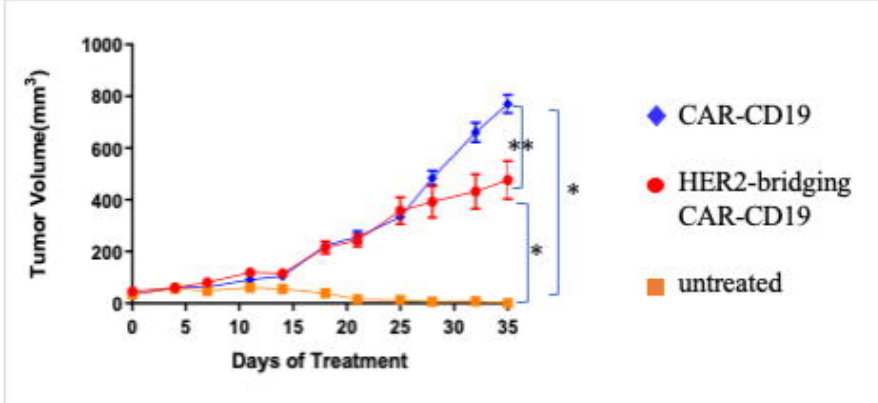

D)

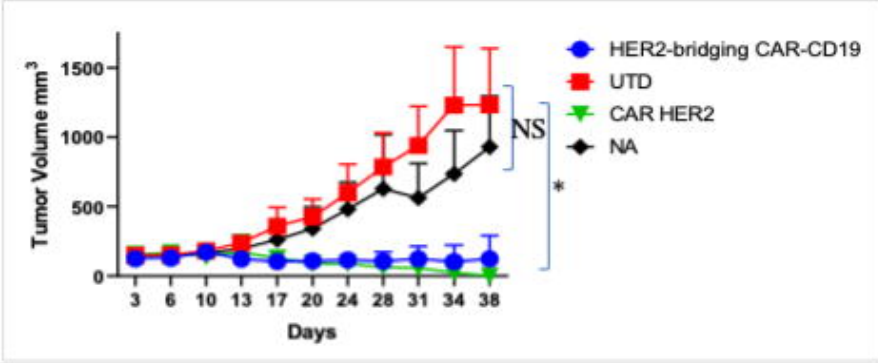

E)

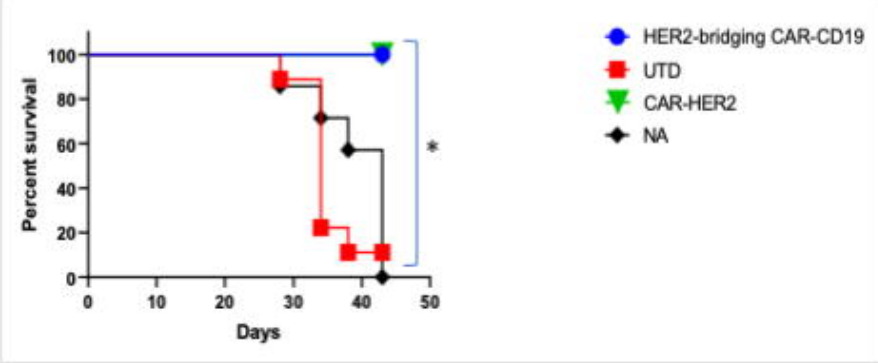

Figure 6.

A)

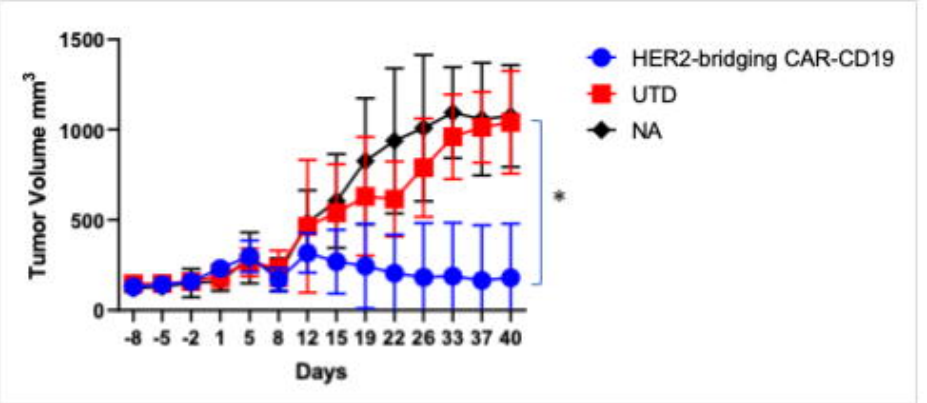
Tumor Volume mm3
1500
1000
500
0
-8 -5 -2 1 5 8 12 15 19 22 26 33 37 40
Days
HER2-bridging CAR-CD19
UTD
NA
*

B)

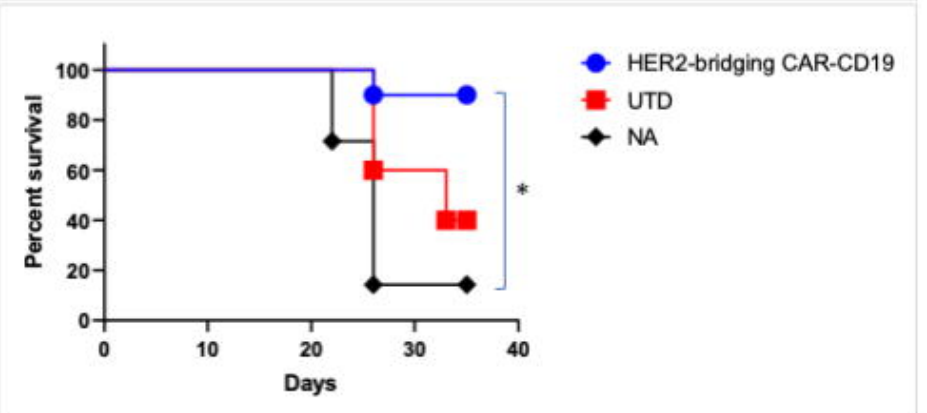
Percent survival
100
80
60
40
20
0
0 10 20 30 40
Days
HER2-bridging CAR-CD19
UTD
NA
*

C)

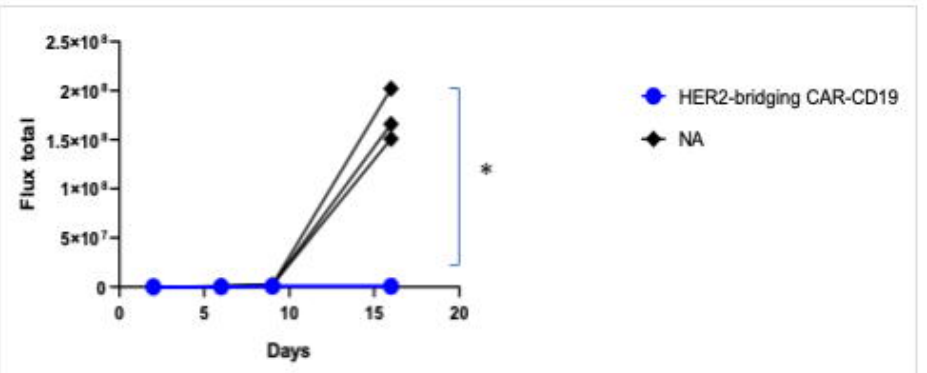
Flux total
2.5×10⁸
2×10⁸
1.5×10⁸
1×10⁸
5×10⁷
0
0 5 10 15 20
Days
HER2-bridging CAR-CD19
NA
*